SMALL SCALE DISCHARGE STUDIES

J. A. Mangano and J. H. Jacob
AVCO EVERETT RESEARCH LABORATORY, INC.
2385 Revere Beach Parkway
Everett, MA 02149

Semi Annual Report for Period 1 September 1974 to 28 February 1975

Sponsored by
DEFENSE ADVANCED RESEARCH PROJECTS AGENCY
ARPA Order No. 1806

Monitored by
OFFICE OF NAVAL RESEARCH
DEPARTMENT OF NAVY
Arlington, VA 22217

FOREWORD

ARPA Order No.: 1806

Program Code No.: 5E20

Name of Contractor: Avco Everett Research Laboratory, Inc.

Effective Date of Contract: 15 August 1974

Contract Expiration Date: 14 August 1975

Amount of Contract: $201,840

Contract No.: N00014-75-C-0062

Principal Investigator and Phone No.: J.A. Mangano
(617) 389-3000, Ext. 725

Scientific Officer: Director, Physics Program, Physical Sciences Division
Office of Naval Research
Department of Navy
800 North Quincy Street
Arlington, VA. 22217

Short Title of Work: Laser Discharge Studies

UNCLASSIFIED

SECURITY CLASSIFICATION OF THIS PAGE (When Data Entered)

REPORT DOCUMENTATION PAGE

READ INSTRUCTIONS BEFORE COMPLETING FORM

1. REPORT NUMBER

2. GOVT ACCESSION NO.

3. RECIPIENT'S CATALOG NUMBER

4. TITLE (and Subtitle)

(6) SMALL SCALE DISCHARGE STUDIES,

(9) 5. TYPE OF REPORT & PERIOD COVERED
Semi Annual rept.
September 74 — Feb 75

6. PERFORMING ORG. REPORT NUMBER

7. AUTHOR(s)

(10) J.A. Mangano and J.H. Jacob

(15) 8. CONTRACT OR GRANT NUMBER(s)
N00014-75-C-0062

9. PERFORMING ORGANIZATION NAME AND ADDRESS
Avco Everett Research Laboratory, Inc.
2385 Revere Beach Parkway
Everett, Massachusetts 02149

10. PROGRAM ELEMENT, PROJECT, TASK AREA & WORK UNIT NUMBERS
DARPA Order - 1806

11. CONTROLLING OFFICE NAME AND ADDRESS
Defense Advanced Research Projects Agency
ARPA Order No. 1806

12. REPORT DATE
(11) Feb 75

13. NUMBER OF PAGES
37

14. MONITORING AGENCY NAME & ADDRESS (if different from Controlling Office)
Office of Naval Research
Department of Navy
Arlington, VA. 22217

15. SECURITY CLASS. (of this report)
UNCLASSIFIED

15a. DECLASSIFICATION/DOWNGRADING SCHEDULE

16. DISTRIBUTION STATEMENT (of this Report)

Approved for public release; distribution unlimited.

(12) 34 p.

17. DISTRIBUTION STATEMENT (of the abstract entered in Block 20, if different from Report)

18. SUPPLEMENTARY NOTES

19. KEY WORDS (Continue on reverse side if necessary and identify by block number)
1. Visible/UV Lasers
2. High Pressure Discharges

20. ABSTRACT (Continue on reverse side if necessary and identify by block number)

In this report we have investigated the possibility of building high power visible and UV lasers. A likely method of scaling visible lasers to high average powers is by e-beam controlled discharges. In the six months between September 1974 to March 1975, we have investigated the discharge physics of Ar/N_2, N_2/NO and SF_6/N_2 mixtures. These laser mixtures were chosen because they effectively cover the wide variety of discharge conditions one is apt to encounter.

* has been investigated

DD FORM 1 JAN 73 1473 EDITION OF 1 NOV 65 IS OBSOLETE

UNCLASSIFIED

SECURITY CLASSIFICATION OF THIS PAGE (When Data Entered)

048450

TABLE OF CONTENTS

LIST OF ILLUSTRATIONS

I. INTRODUCTION

The major objective of the proposed program is to demonstrate that the e-beam stabilized discharge can be used as a scalable, efficient visible or UV laser pumping method. This objective was accomplished by using this discharge method to pump potentially high power, efficient laser mixtures. The mixtures included Ar/N_2,[1,2] N_2/NO,[3] and SF_6/N_2.[4] These laser mixtures were chosen because they effectively cover the wide variety of discharge conditions one is apt to encounter. For example, the Ar/N_2 system is representative of laser mixtures whose discharge physics is dominated by the rare gases. The N_2/NO system, on the other hand, is representative of laser mixtures whose discharge properties are dominated by molecules (vibrational excitation, etc.). Finally, discharges made in SF_6/N_2 are typical of those dominated by attachment. Hence a wide spectrum of discharge conditions is encountered in working with these laser mixtures.

---

(1) Bhaumik, M. and Ault, E., IEEE J. Quant. El. 624, 10, (1974).

(2) Searles, S., NRL, to appear in App. Phys. Lett.

(3) Ewing, J. J. and Yatsiv, S., Avco Everett Research Laboratory, Inc. LAR Proposal (1972).

(4) Suchard, S., Aerospace, private communication.

II. DISCHARGE PUMPING OF VISIBLE LASERS

Discharge pumping could result in a high efficiency ($\geq 10\%$), high average power ($\geq$ 100 kW), visible laser. Discharge pumping requires deposition of large energy densities at the proper E/P. The applied electric field should be strong enough such that the electron temperature is $\geq$ 3 eV. At these electron temperatures the ionization rate is high, typically 10^7 -10^8 sec^{-1}. As a result the discharge current e-folds every 10-100 nsec and it is difficult to maintain discharge stability for the duration of the discharge pulse time.

We have developed a program to determine if discharges can be used to pump visible lasers efficiently. The steps in this program are as follows:

(1) Optimize Cavity Design

In order to optimize laser efficiency and achieve high energy densities, the discharge must typically be operated at the highest electric field possible. It is therefore important to operate with a discharge electric field as close as possible to the intrinsic arcing limit of the laser mi ture. To approach this limit, it is necessary to eliminate electric field stress concentrations associated with the shapes and positions of the discharge electrodes and insulating side walls. For this purpose we have designed a dc/pulsed gas breakdown apparatus. The results and analyses of the experiments performed on this apparatus will be presented below.

(2) Control Discharge Spatial Uniformity

Nonuniform e-beam energy deposition and the resulting nonuniform plasma conductivity can also lead to electric field stress concentrations. Therefore, careful understanding and control of the beam energy deposition in the discharge cavity is necessary. The 150 keV beam built under previous ARPA contracts[5] is sufficiently energetic for our anode/cathode spacing of 2 cm. If greater uniformity is desired, we can delay the discharge pulse with respect to the e-beam pulse. For recombination-dominated discharges this will tend to make the plasma conductivity more uniform, minimizing electric field stresses. Results of delaying the discharge pulse with respect to the e-beam will be shown in later sections.

(3) Determine Appropriate E/P for Efficient Pumping

We next have to determine if the E/P is high enough to efficiently pump the upper laser level. At AERL we have a Boltzmann code for this purpose. If all the electron impact cross sections are known, then the code predicts the fraction of energy going into various excited states. We have, by this method, analyzed the Ar/N_2 and N_2/NO laser systems to determine the proper E/P for efficient lasing action.

---

(5) Mangano, J. A., Avco Everett Research Laboratory, Inc. LAR Final Report (1973).

(4) Use of Attaching Species to Stabalize Discharge

For certain laser systems (for example Ar/N_2) we may find it impossible to deposit enough energy at the proper E/P to pump the upper level efficiently. For these systems we will investigate the use of attaching species in an attempt to reduce the net ionization rate. Care must be taken in the use of attachers to prevent interference with the laser kinetics or absorbtion of a significant fraction of discharge energy.

A. OPTIMIZATION OF CAVITY DESIGN (BREAKDOWN EXPERIMENT)

To optimize the laser cavity design we have built a breakdown chamber in which different cross-sectional electrode and insulator shapes can be tested. Presently we are able to perform dc breakdown measurements only. However, modification to enable measurement of pulsed breakdown is underway. The chamber can also be modified to measure ionization rates in different laser gas mixtures. Such information for specific systems is presently unavailable.

A schematic of the breakdown chamber is shown in Figure 1. The upper Rogowski surface is designed for a 1/4 inch spacing above the lower planar electrode. The chamber can be pumped down to base pressures of $\leq 10^{-5}$ torr. We can insert insulators of various shapes as well as introduce screens of various transparencies to simulate the laser discharge cavity.

In Figure 2 examples of breakdown measurements performed on the device are shown. The solid curve with open circle data points is for commercially pure N_2. Our results are within 5% of previously reported data. A straight wall lucite disc was next inserted between the electrodes. Contrary to published results,(6) the breakdown field remained unchanged. This is shown by the open triangle in Figure 2. When we replaced the straight wall insulator by a convex shape lucite insulator, the breakdown electric field dropped by about 20%. For a concave shape lucite insulator the breakdown electric field dropped another 10%. Also shown in Figure 2 is the dc breakdown in our present laser discharge cavity. The shape of the insulating sidewalls in this cavity are concave. Of we cured this cavity the breakdown electric field increased slightly but was still smaller than the electric field in the breakdown experiment for the concave shape insulator. The reason for this difference is that the pd product in our cavity is about 4 times larger than in the breakdown experiment. It is a well established fact that the breakdown electric field decreases slowly with pd.

These results can be explained if one assumes that the N_2 in the gap becomes conducting just before breakdown. This assumption is substantiated by experiments showing that microamps/cm^2 of current generally flow before breakdown occurs. The currents charge up the insulating surface and force the electric field lines at the interface surface to flow parallel to the surface of the insulator. As a result the electric field concentrates near discontinuities in the insulator surface.

---

(6) Cobine, J. D., Gaseous Conductors, Dover Pub., p. 166 (1957).

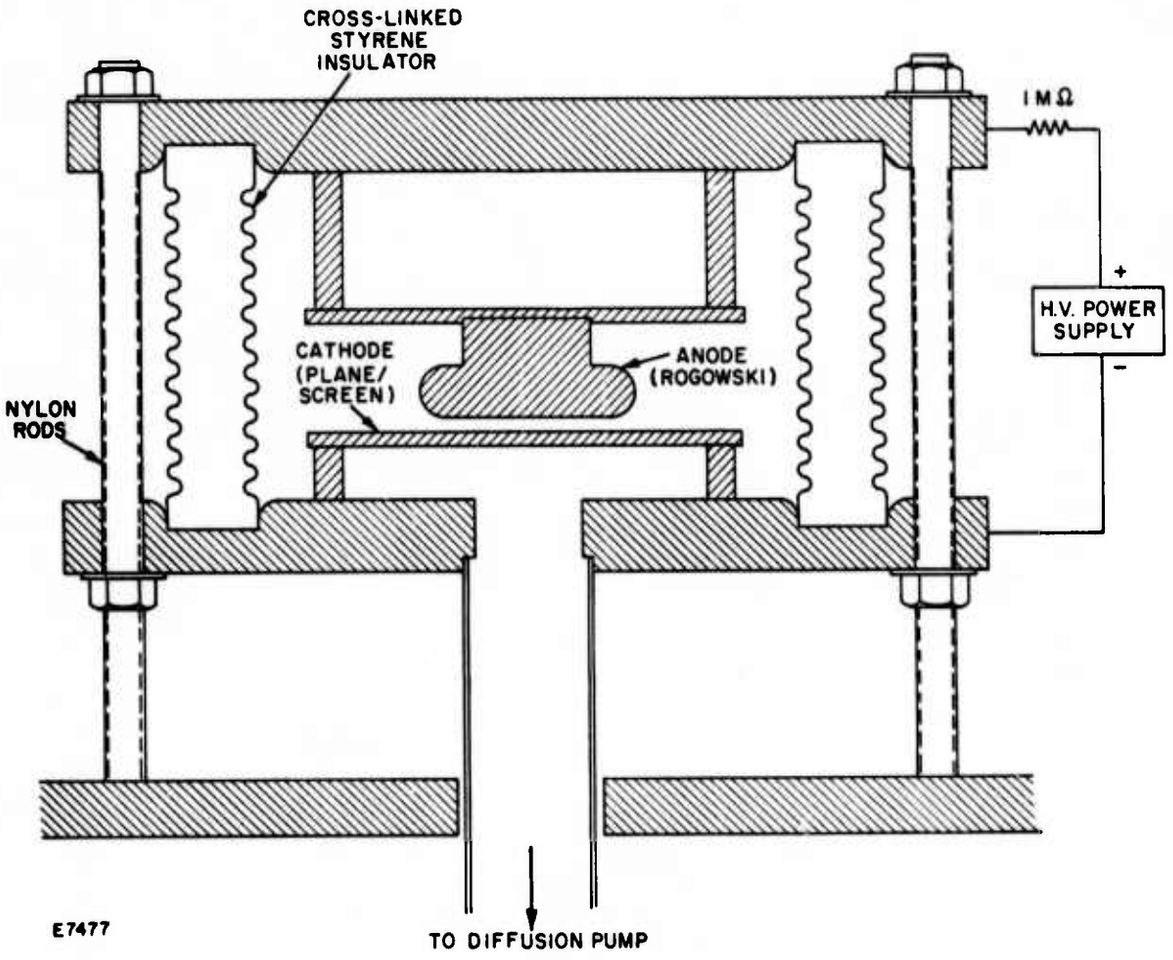

Figure 1 Cross-Sectional View of the Breakdown Experiment

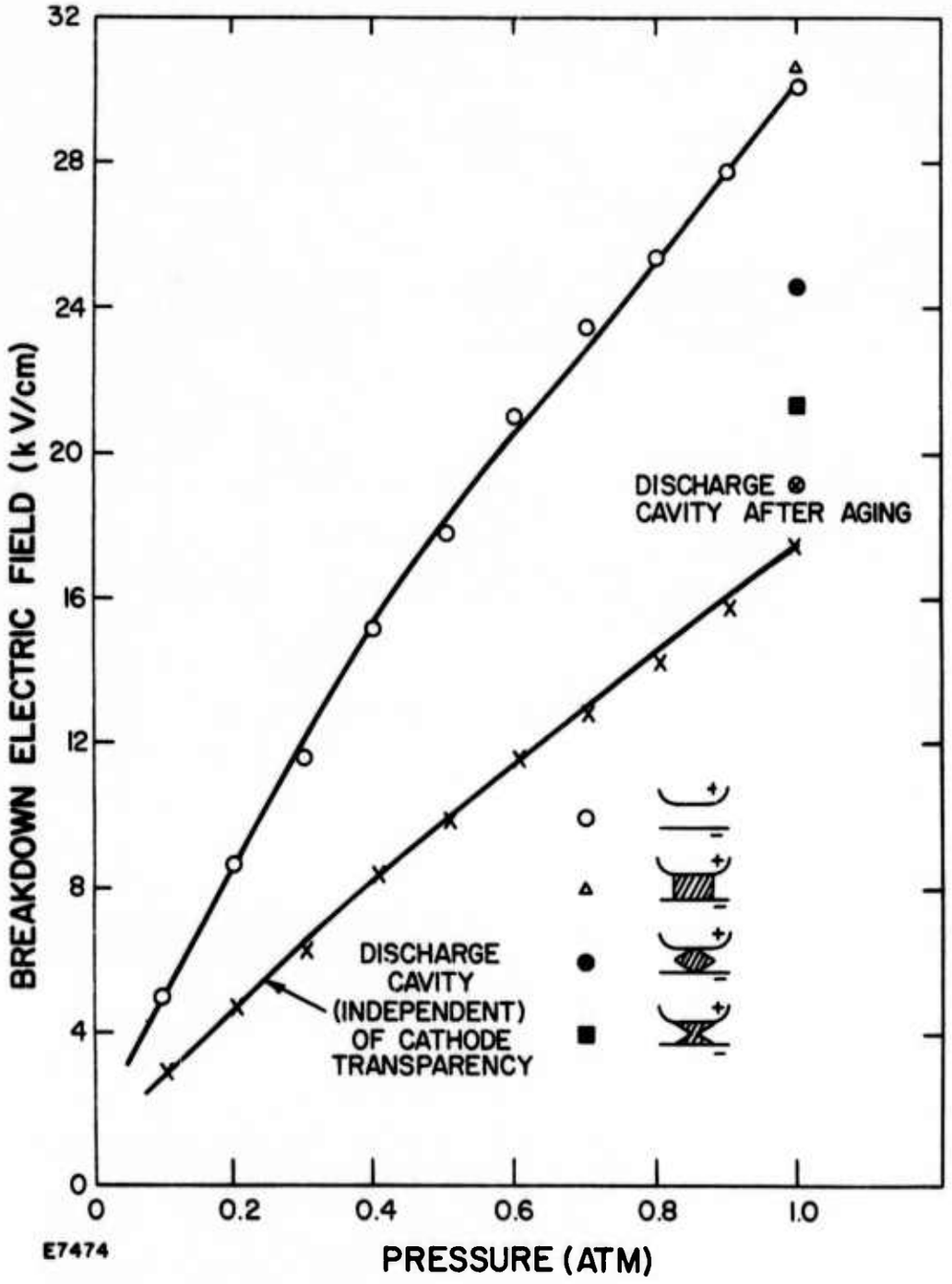

Figure 2 Results of Breakdown Measurements Taken in Commercially Pure N_2. Notice that straight wall insulators do not appreciably alter the breakdown electric field. Also shown are the breakdown characteristics in the discharge cavity.

This point is clearly seen in the computer plot shown in Figure 3. In this figure the equipotential lines for one-quarter of the discharge cavity are shown. The spacing between the lines is a direct measure of the electric field strength. It is clear from Figure 3 that the electric field is much stronger at one of the insulator-metal junctions. So when the average electric field is near breakdown one of the corners has an electric field that is larger than the breakdown value. This will cause the gas to breakdown and arc from the corner of the dielectric. The average electric field amplitude at which we can operate stably is thereby reduced. If the insulator surface is normal to the plane of the electrodes the electric field will be uniform and the breakdown characteristic unchanged. So it appears that if insulating walls are necessary in the discharge cavity they should be normal to the electrode surface.

B. CONTROL OF DISCHARGE SPATIAL UNIFORMITY

The initial uniformity of the plasma conductivity is controlled to a large extent by the unfiromity of the e-beam energy deposition. Our e-beam has an energy of 150 keV. Because of the strong dependency of the scattering and energy loss on the atomic number Z, it is advantageous to use a low Z foil. The foil should also be strong enough to support a pressure difference of 15 psia across it. Kapton has a average Z of about ~ 6 and we have found that 1 mil of Kapton is easily capable of supporting one atmosphere pressure across it even with an 80% open foil support structure. However, when large amounts of energy are stored in the discharge circuitry ($\geq$ 1 kJ), and small foil to cathode screen spacings are used, 2 mil kapton foils are necessary. The increased strength is required to handle the large local overpressures associated with discharge arcs.

Figure 4 shows thepredicted distribution function of the electrons after passing through 1 and 2 mil kapton foils. The half-width of the angular distribution function increases from 17° for a 1 mil foil to 27° for a 2 mil foil. Figures 5 and 6 show the results of assuming that the electrons freestream after passing through the foil. In these figures we have plotted contours of constant energy deposition. The energy deposition is normalized to unity at the foil surface that extends between $-1 \leq y \leq 1$. There is a 10% variation between contours. The streaming approximation is good provided that the anode/cathode spacing divided by the transport mean free path < 0.2. In pure nitrogen, argon and xenon, these ratios are 0.055, 0.148 and 1.2 respectively. So the streaming approximation is good for nitrogen, acceptable for argon, while for Xe we have to include the effects of scattering. Figure 7 shows the result of including the effects of scattering and energy loss when the cavity is filled with pure Xe. We have assumed that the electrons leaving the foil are diffuse in angle. This assumption is good for the 2 mil foil. For the 1 mil foil the energy deposition contours will extend 5-10% further out from the beam entrance plane. It is clear from Figure 7 that our e-beam is not sufficiently energetic to uniformly ionize an atmosphere of pure Xe in our 2 cm wide cavity.

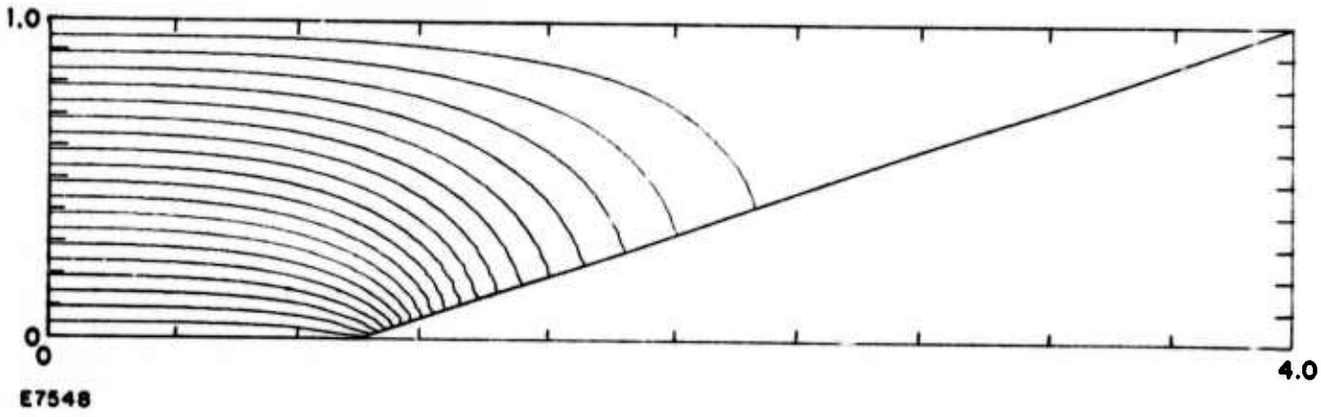

Figure 3 Computer Plot of Equipotential Contours for a Concave-Shaped Insulator. The spacing between contours is a direct measure of the electric field strength.

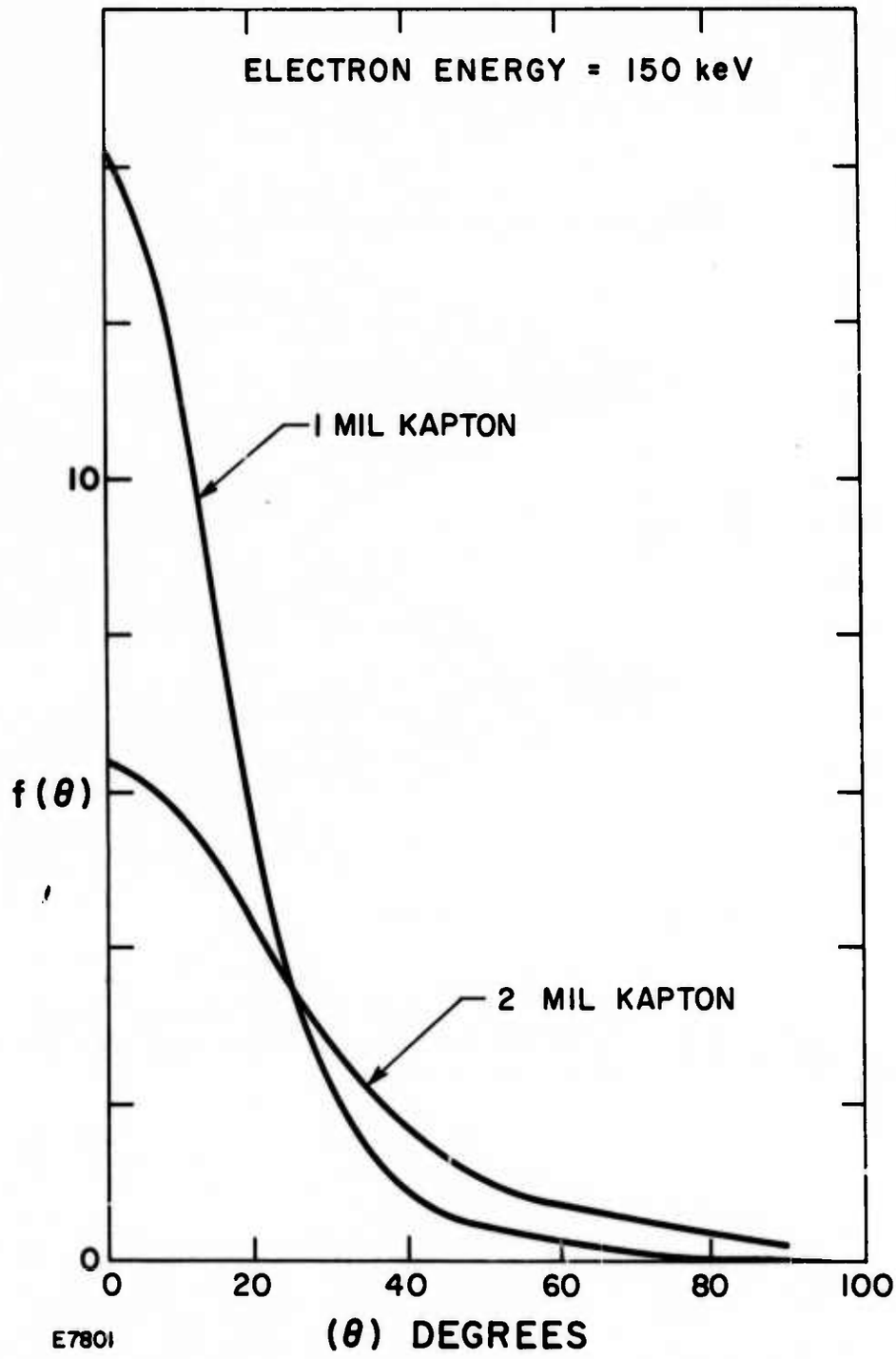

Figure 4 Plot of the Angular Distribution for Electrons Emanating From 1 and 2 mil Kapton Foils. The initial energy is 150 keV.

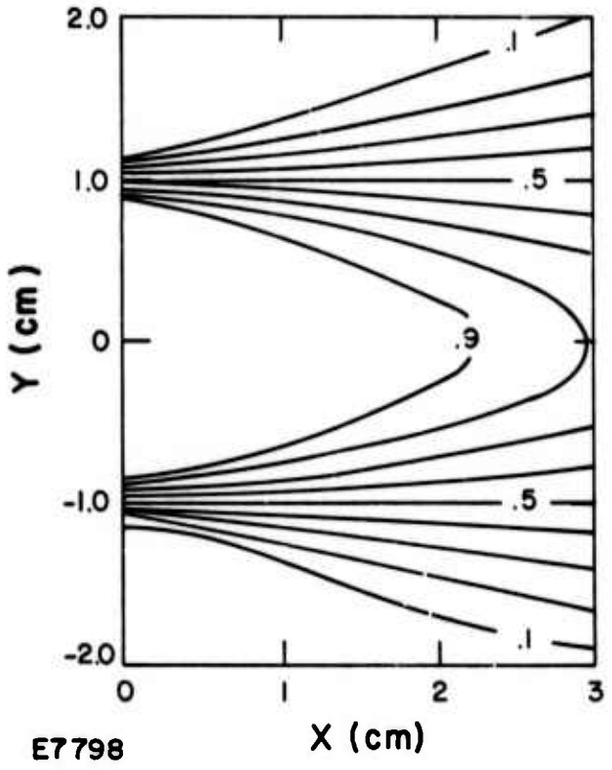

Figure 5 Contours of Energy Deposition by a High Energy E-Beam After Traversing a 1 mil Kapton Foil. We have neglected effects of inelastic and elastic gas scattering.

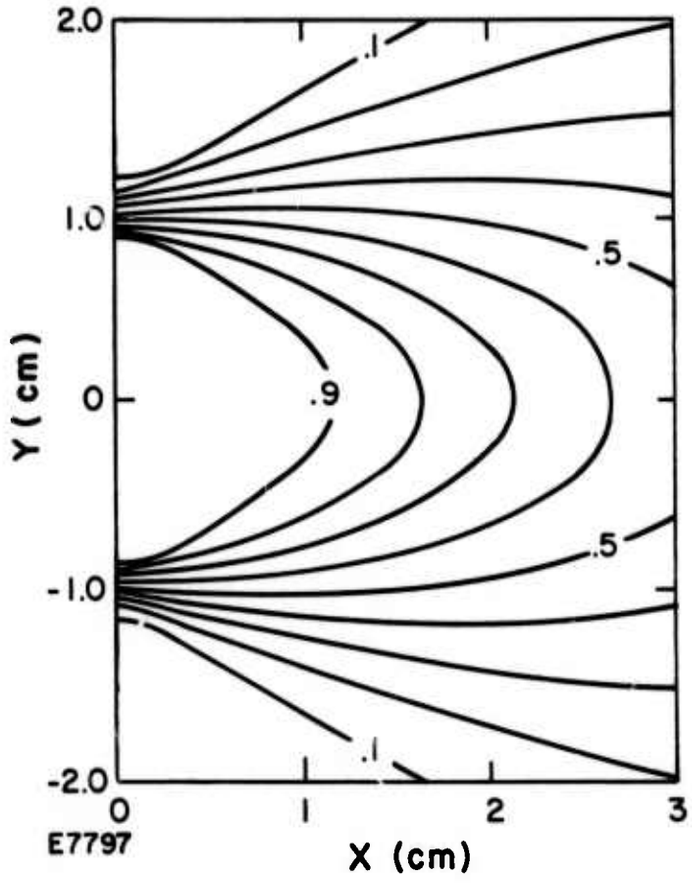

Figure 6 Same as Figure 5 Except that we have Assumed that the Electrons Pass Through a 2 mil Kapton Foil

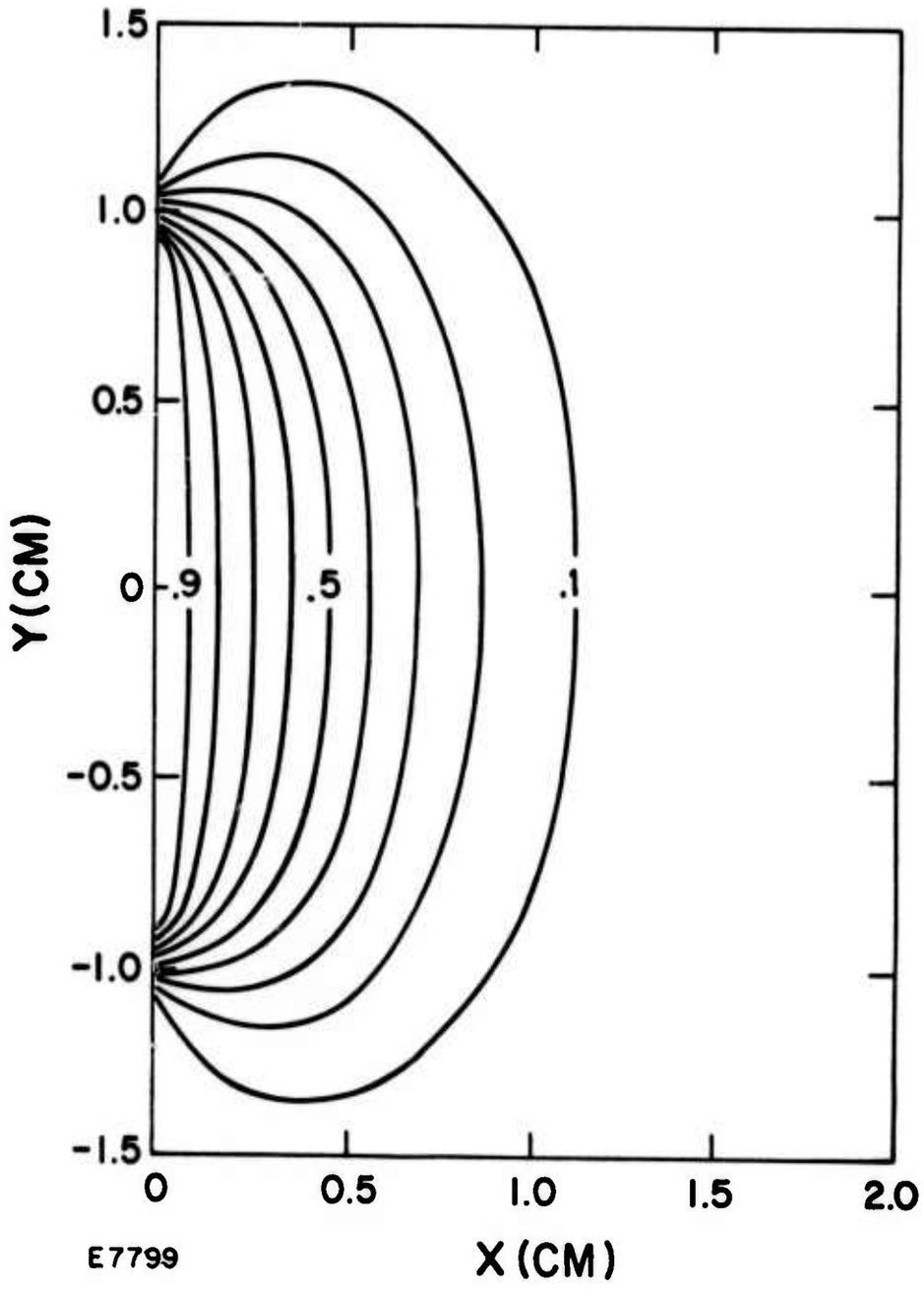

Figure 7 Contours of Energy Deposition for the Special Case of Xenon. We have included effects of both inelastic and elastic scattering.

If we want even greater discharge uniformity we can delay applying the discharge voltage with respect to the e-beam pulse. In a recombination-dominated discharge this will make the plasma conductivity more uniform since the electrons will tend to recombine more rapidly in the regions of higher electron density. For example, in Ar/N_2 discharges we found that delaying the discharge was necessary to achieve the required electric field of 10 kV/cm atm. Another advantage of applying the discharge voltage after the e-beam is turned off is that we increase the volumetric scalability of the discharge. This increase results from the absence (during the e-beam pulse) of the magentic field associated with the discharge current. The magnetic field, if strong enough, will cause the e-beam to pinch on itself in the discharge cavity.

C. DETERMINE REQUIRED E/P

The next steps in applying discharge pumping to a given laser gas mixture are:

1) Determine the E/P necessary for efficient pumping of the desired electronic state

2) Determine the energy density that can be deposited during the stable portion of the discharge pulse at this E/P

This information can be supplied in part by the AERL Boltzmann code if the relevant electron impact cross sections are known. Given these cross sections, this code yields the rates of pumping the various excited states, the ionization rate and the electron drift velocity as a function of E/P for arbitrary gas mixtures. The discharge energy partitioning into each of these proceses is also given. Therefore, with this code the E/P required for inverting a given transition can be determined as well as the efficiency of generating the inversion.

The pulse duration for which discharge stability can be maintained at the required E/P must then be found. This pulse duration will be a function of the preionization level and the ionization rate. However, at present, a reliable short time discharge stability theory, which gives discharge stability duration as a function of these parameters, does not exist. In fact development of such a theory is a part of the ongoing effort of the Laser Discharge Studies Program. Consequently, we are forced to determine this pulse duration for a given laser mixture experimentally. Together with construction of the discharge apparatus, gathering os such discharge data for the Ar/N_2, $N_2(A)/NO$ and SF_6/N_2 laser systems represented themajor part of the discharge studies program for FY75.

Of course once this stable pulse duration has been found for the required E/P and preionization level, the total discharge energy density input to the laser mixture is known. The Boltzmann code results and the relevant laser kinetics code can then be used to predict overall laser efficiency and laser output energy density.

In this section, the procedure outlined above will be demonstrated for discharge pumpint of the Ar/N_2 and $N_2(A)/NO$ laser systems.

1. The Ar/N_2 Laser

Figure 8 shows a diagram of the relevent energy levels of Ar and N_2. High intensity e-beam pumping of this laser depends on the formation of Ar^+. Approximately one half of the beam energy deposited in the laser mixture is channeled into Ar^+ production. The remaining energy is widely distributed among other excited states. The argon ions produced rapidly form molecular ions which dissociatively recombine to form Ar^*. These argon mestastables then transfer about 40% of their energy to N_2 (C, v = 0) - the upper laser level. The lower laser level is the N_2 (B, v = 1) state.

With discharge pumping of this laser, Ar^* would be formed directly by electron impact.* This pumping method can be efficient as long as

1) Stable operation at electric fields high enough to make Ar^* efficiently can be achieved

2) Stable operation at electric fields high enough to prevent significant population of N_2 (B, v = 1) can be achieved

3) Ionization of the argon metastables at the required Ar^* density and E/P does not interfere substantially with laser kinetics and/or maintenance of discharge stability.

Figure 10 shows a plot of the fraction of discharge energy that is deposited into various excited states in a 97% Ar/3% N_2 mix as predicted by the Boltzmann code. The maximum possible efficiency of producing Ar^* in an e-beam is about 40%. This means that if we are to pump Ar^* in a discharge with the same efficiency as with an e-beam we should operate at electric fields of at least 10 kV/cm atm. At these electric fields the fraction of discharge energy going into the N_2(B) is about 16%. However, only 4% of the discharge energy is deposited into the v = 1 vibrational level of N_2(B) (if the energy into vibration partitions itself according to the Franck-Condon factors). So it appears that if we can operate our discharge stably at electric fields of 10 kV/cm atm and deposit about 10 J/liter atm into Ar^* production in 50 nsec, Ar/N_2 will lase in a discharge.

---

*The electron impact cross sections of Ar^* have not been measured since 1935.(7) The relative magnitude of the total Ar^* cross section as a function of energy has been measured recently by Olmsted et al.(8) To estimate the absolute magnitude of these cross sections we took Olmsted's relative cross section and varied its absolute value until we reproduced the first Townsend coefficient as measured by Golden et al.(9) Figure 9 shows the sensitivity of α to the magnitude of the Ar^* cross section. Varying the magnitude of the metastable cross section by a factor of 3 resulted in almost two orders of magnitude variation in α. The ionization cross sections have recently been measured by Rapp et al.(10)

(7) MacDonald, A. D., Microwave Breakdown in Gases, Wiley Pub., p. 25 (1966).

(8) Olmstead, J., Newton, A. S. and Street, I. E., J. Chem. Phys. 42, 2321 (1965).

(9) Golden, D. E., Fisher, L. H., Phys. Rev. 123, 1079 (1961).

(10) Rapp, D., Englander-Golden, P., J. Chem. Phys. 43, 1464 (1965).

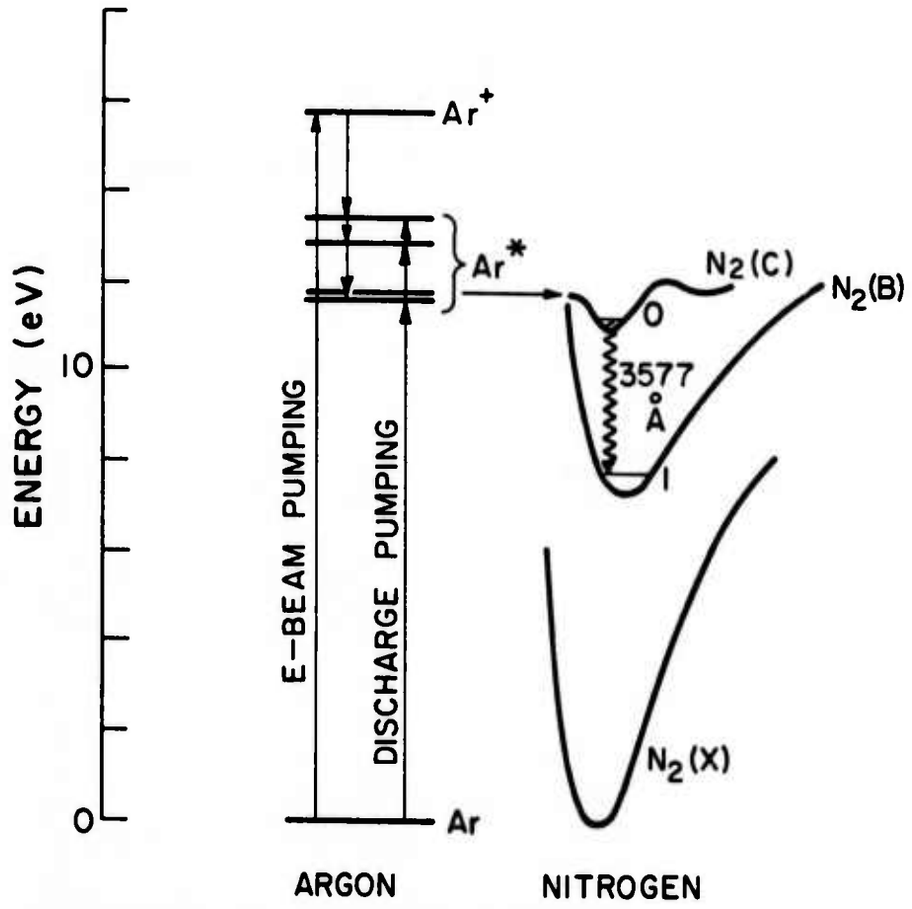

Figure 8 Schematic of the Energy Levels in Ar and N_2

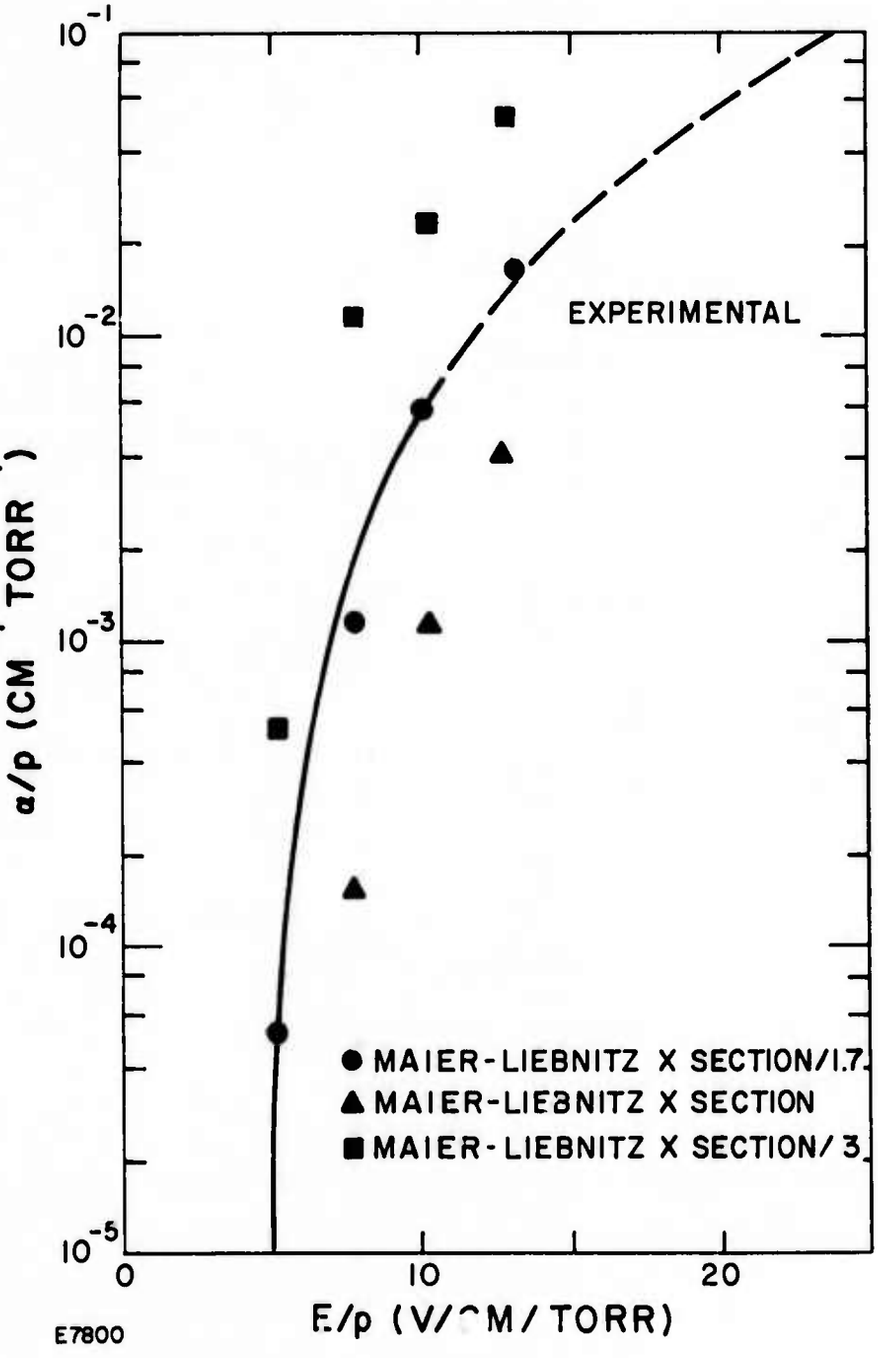

Figure 9 Plot Demonstrating the Sensitivity of the First Townsend Coefficient as a Function of E/p for Different Values of the Metastable Cross Section. The best fit to the experimental data is Maier-Libneitz results divided by 1.7.

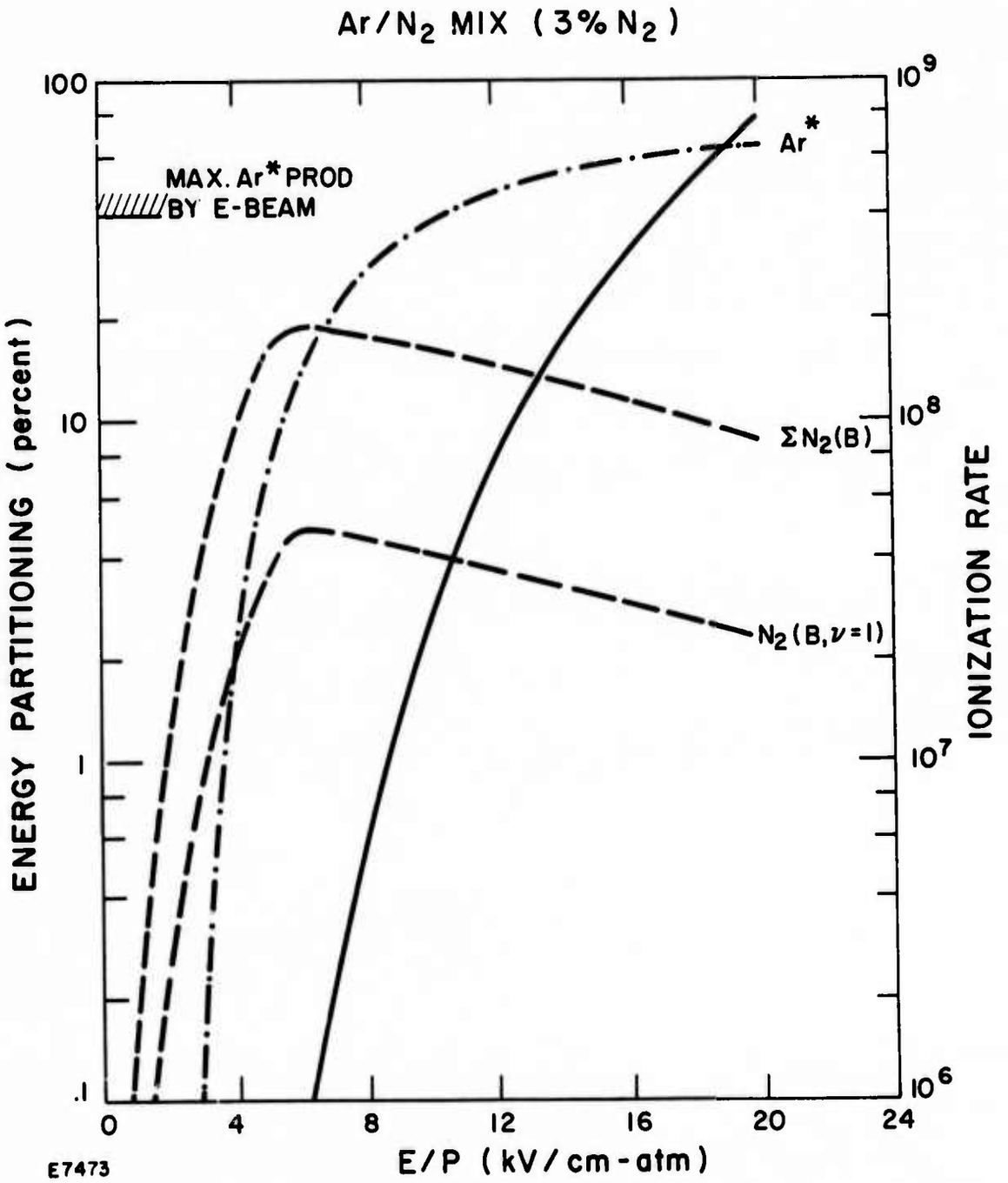

Figure 10 Fraction of Discharge Energy Into Various Excited States of Ar and N_2 as Predicted by the Boltzmann Code. Note that to pump Ar^* in discharge with an efficiency comparable to that achieved with an e-beam we need an E/p of 10 kV/cm atm.

In the solution of the Boltzmann equation we have neglected electron impact excitation and ionization of the Ar^* and other excited species. Since Ar^* is atomically similar to potassium, the ionization rate constant of the Ar^* should be $\approx 5 \times 10^{-8}$ cm^3/sec for electron temperatures of ~ 4 eV. As a result theionization rate of the Ar^* becomes comparable to the ionization rate of Ar for a metastable density of 10^{15}/cm^3. As we require about this density of Ar^* to lase Ar/N_2, metastable ionization is clearly important. Further the presence of this comparatively large cross section with a 4 eV threshold could lower the electron temperature. In the FY76 program we will include effects of Ar^* excitation and ionization by electron impact in the Boltzmann code so that these effects on laser kinetics, discharge stability and required E/P can be assessed.

The kinetic equations describing a discharge pumped Ar/N_2 laser are:

$$\frac{d\,Ar^+}{dt} = S_{eb} + \nu_1\,(Ar)\,n_e + \nu_2\,(Ar^*)\,n_e - k_1\,(Ar)^2\,(Ar^+) \qquad (1)$$

$$\frac{d\,Ar_2^+}{dt} = k_1\,(Ar)^2\,Ar^+ - \alpha\,[Ar_2^+]\,n_e \qquad (2)$$

$$\frac{d\,Ar^*}{dt} = k_2\,Ar\,[Ar_2^+]\,[n_e] - \nu_2\,n_e\,Ar^* - k_3\,N_2\,Ar^* \qquad (3)$$

$$\frac{d\,N_2\,(C)}{dt} = 0.4\,k_3\,N_2\,Ar^* - \frac{N_2\,(C)}{t_c} - k_4\,N_2\,N_2\,(C) \qquad (4)$$

where $n_e = Ar_2^+ + Ar^+$. Equation (1) describes the production and loss of Ar^+. The argon ions rapidly form molecular ions via a three body process ($k_1 \approx 2.5 \times 10^{-3}$ cm^6/sec). ν_1 and ν_2 are the ionization rate constants of Ar^+ and Ar^* by discharge electrons and S_{eb} is the beam electron ionization source term. The time evolution of Ar_2^+ is described by Eq. (2). In writing Eq. (2) we have assumed quasi-neutrality i.e., the electron density is equal to $[Ar_2^+ + Ar^+]$. The Ar_2^+ dissociatively recombines to form Ar^*. The recombination rate is very temperature dependent. For 300° K electrons $\alpha = 10^{-6}$ cm^3/sec. Equation (3) describes the production and loss rate of Ar^*. k_2 is the production rate of Ar^* by direct electron impact and k_3 is the quenching rate of the metastables by N_2. Finally Eq. (4) describes the production and loss rate of $N_2(C)$. The 0.4 in the first term on the RHS of (4)

accounts for the fact that only 40% of the energy goes into forming $N_2(C)$. t_c is the spontaneous emission of the C-state and k_4 is the deactivation rate for $N_2(C)$ by N_2.

2. Discharge Experiments in Ar/N_2

Discharge experiments in Ar/N_2 mixtures indicated that the required E/P of 10 kV/cm atm could not be obtained if the discharge voltage was switched on simultaneously with the e-beam pulse. When the discharge voltage was delayed we could obtain an electric field of the order of 10 kV/cm atm. Figure 11 shows the results of such a delay. In this case the e-beam current density in the laser mixture was 0.6 A/cm^2. The fluorescent at 3577 Å was detected by a 1/4-meter Jarrel Ash spectrometer. Looking at Figure 11 we see enhancement of the fluorescence by the discharge as compared to the e-beam. Also the discharge current is clearly exponentiating until it arcs. The fluorescence also increases rapidly after the discharge voltage is turned on. In fact, during the stable part of the discharge pulse its shape is similar to the discharge current. After arcing the discharge voltage drops rapidly. The efficiency of pumping Ar^* is considerably smaller and, as a result, the fluorescence decreases. The subsequent increase in PM signal is the result of noise from the arc. The electric field for the run shown in Figure 11 was about 6 kV/cm atm, and the discharge energy deposited before arcing was about 5 J/liter. We were also able to achieve the required electric field of 10 kV/cm atm. However, the energy deposited by the discharge was only 2.5 J/liter. This lowering of the input discharge energy was caused by a decrease in the time for which the discharge remained stable.

3. N_2/NO Laser

Figure 12 is a schematic energy level diagram of the N_2/NO laser. For this laser system we would like to create $N_2(A)$ in a discharge and transfer this energy to NO(A). The laser transitions are the NO γ-bands in which lasing action has not yet been demonstrated. Demonstration of lasing action will require a relatively large inversion density because of small transition probabilities. The gain is about a factor of 25 lower than the Ar/N_2 laser for a given inversion density. However, low gain means high energy storage and high average power capability.

In Figure 13 the predictions of the Boltzmann code for 3 torr NO in an atmosphere of N_2 are given. Most of the energy in the electronic levels of N_2 will end up in the $N_2(A)$. So it appears that at electric fields of 25 kV/cm atm the efficiency of producing $N_2(A)$ states by discharge pumping is 30-40%. The $N_2(A)$ state can also be pumped indirectly by an e-beam in Ar/N_2 mixtures. Here as in the Ar/N_2 laser case the e-beam produces Ar^+ which rapidly forms the molecular ion Ar_2^+ and then dissociatively recombines to form Ar^*. The Ar^* then transfers to the $N_2(A)$ state. The efficiency of this indirect process is approximately 20%.

In Table I we see a summay of a possible N_2/NO laser system. In arriving at the 6-8% overall efficiency we have used the predicted efficiency

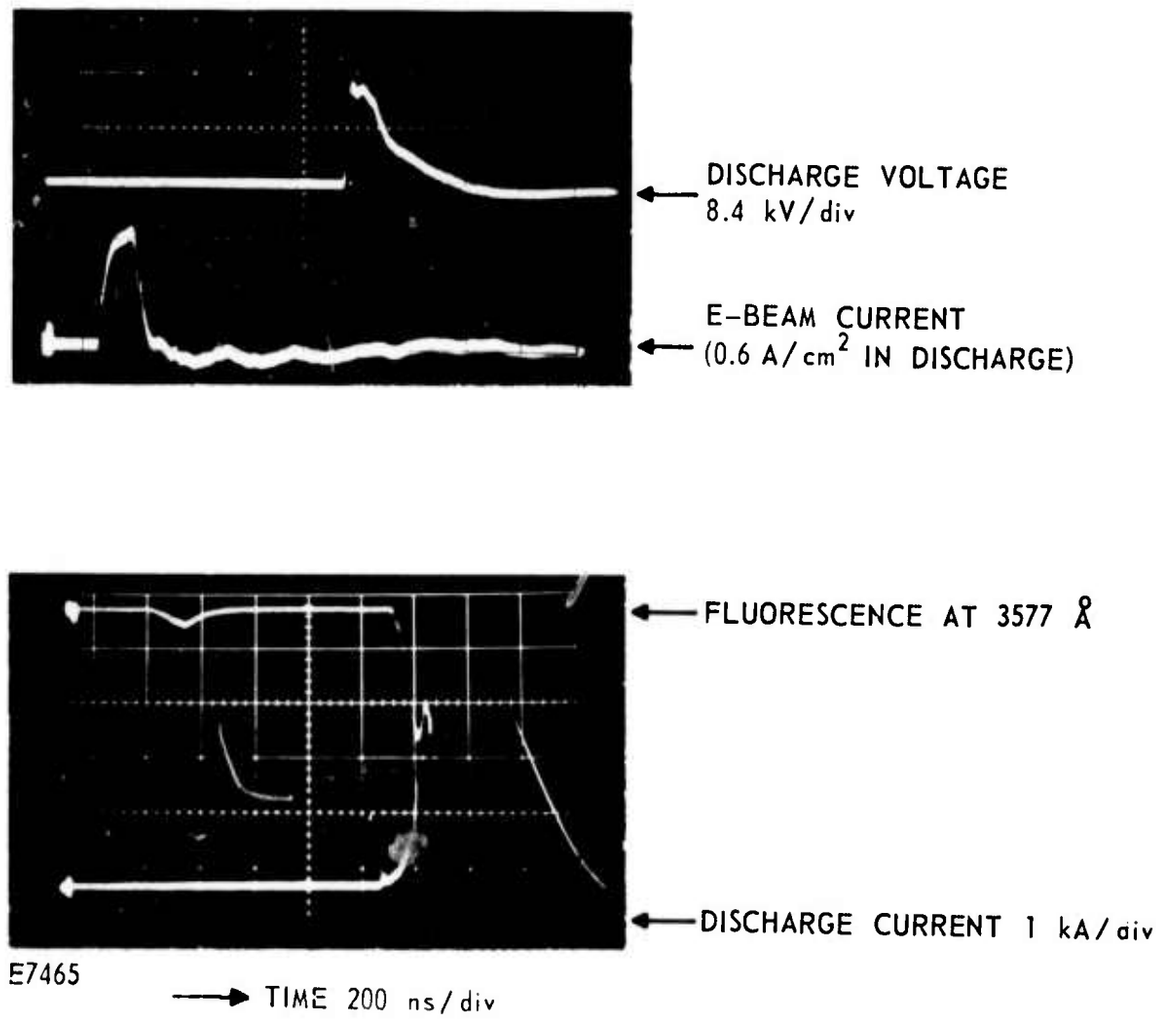

Figure 11 Experimental Results in Ar/N_2 Discharge

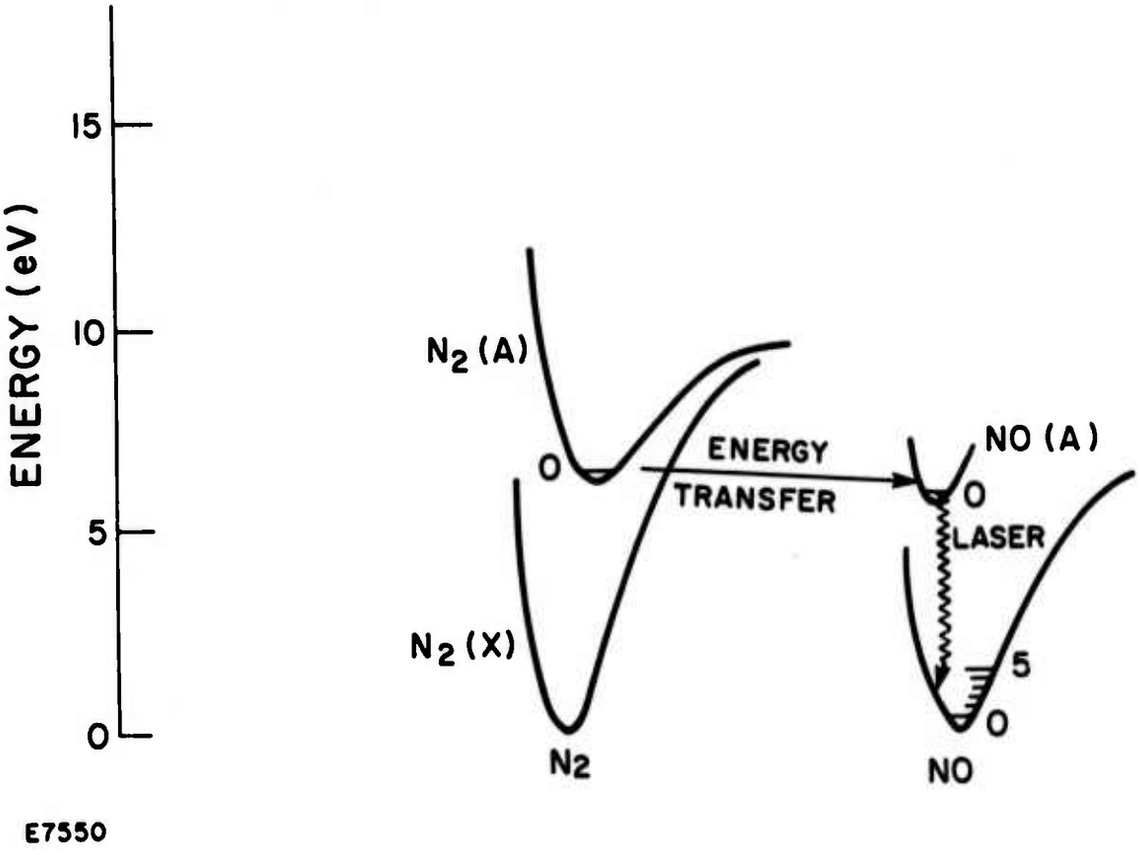

Figure 12 Schematic of Energy Levels in N_2/NO

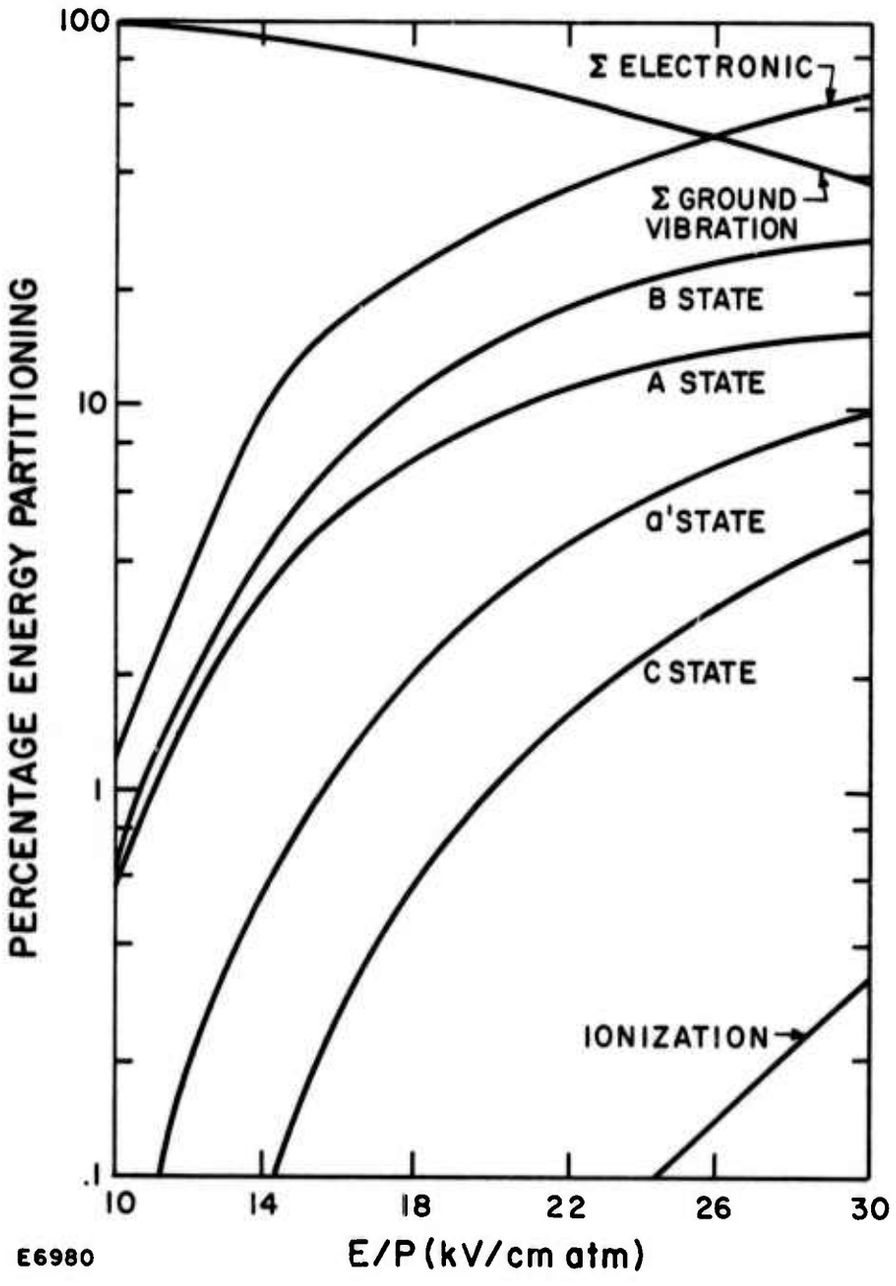

Figure 13 Fraction of Discharge Energy Into Various Excited States of N_2 as a Function of E/p as Predicted by the Boltzmann Code

TABLE I

NO γ -BAND LASER

Wavelength	~2360 Å - 2850 Å
Low Gain	~0.4 - 3 x 10^{17} N_o
Gas Mixture	~3 torr NO - 757 torr N_2
Electric Field	~25-30 kV/cm atm
Discharge Current	~100 A/cm^2
Pulse Length	~150-200 nsec
Possible Efficiency	~6-8%
Energy Out	~20-30 J/liter atm

of 30% for producing $N_2(A)$ in a discharge. According to SRI 50% of all $N_2(A)/NO(X)$ reactions end up in NO(A). If we assume that the laser bottlenecks the efficiency will be reduced another factor of two. The quantum efficiency is 90%. As a result the efficiency of the NO γ-band laser is just 1/4 the efficiency of producing $N_2(A)$.*

4. Experimental Results in N_2/NO

Figure 14 shows typical N_2/NO discharge data. The mixture contained 3 torr of NO in an atmosphere of N_2. For the run shown in Figure 14 the electric field obtained for the first 150 nsec was slightly > 25 kV/cm atm. The mean discharge current at this electric field was about 100 A/cm^2 and the energy deposited in the gas was 375 J/liter. The initial voltage drop is due to the capacitor discharging. An arc occurred about 500 nsec after the discharge voltage was applies. This indicates that we could put in an even greater amount of energy at these voltages. In Figure 14 we also see the fluorescence at 2362 Å corresponding to the NO (A, v = 0) → NO (X, v = 1) transition. The fluorescence increased when the voltage is turned on and begins to decay as the discharge voltage decreases. The second increase in the signal is noise from the arc. Notice that the time scales in theupper and lower photographs are 100 nsec/div and 200 nsec/div respectively.

Finally in Figure 15 we see a time-averaged spectrum of the light from the N_2/NO discharge. It is apparent from this figure that most of the radiated energy emanates in the γ-bands of NO indicating efficient transfer from $N_2(A)$ to NO(A). The NO (A, v = 0) → NO (X, v = 0) is faint because the photographic plate is extremely insensitive below 2300 Å. Also shown in Figure 15 for the purpose of precise wavelength calibration, is a mercury spectrum.

D. EFFECT OF ATTACHERS ON DISCHARGE STABILITY

In Ar/N_2 mixtures we found that we could not deposit enough energy at the required electric field of 10 kV/cm atm. At this electric field the secondary electron ionization rate was about 3.5×10^7 sec^{-1}, i.e., the discharge current increased by e in 28 nsec. This rapid ionization rate led to discharge arcing before significant discharge energy could be deposited. One possibility of stabilizing the ionization rate is to introduce an attacher into the discharge. It is important that the attacher concentration be small enough so as not to interfere with laser kinetics or absorb appreciable energy from the discharge. The latter criteria could be determined

*This assumes that the stimulated deactivation of NO(A) dominates the collisional deactivation by NO(X). If we achieve the predicted 20-30 J/liter in a 100 nsec pulse the stimulated deactivation rate is $\geq 5 \times 10^{23}$ cm^3/sec. This compares to a collisional deactivation rate of 2×10^{22} cm^3/sec in the presence of $10^{17}/cm^3$ of NO. We have also assumed that the rate of pumping the ground state vibrational levels of NO is negligible.

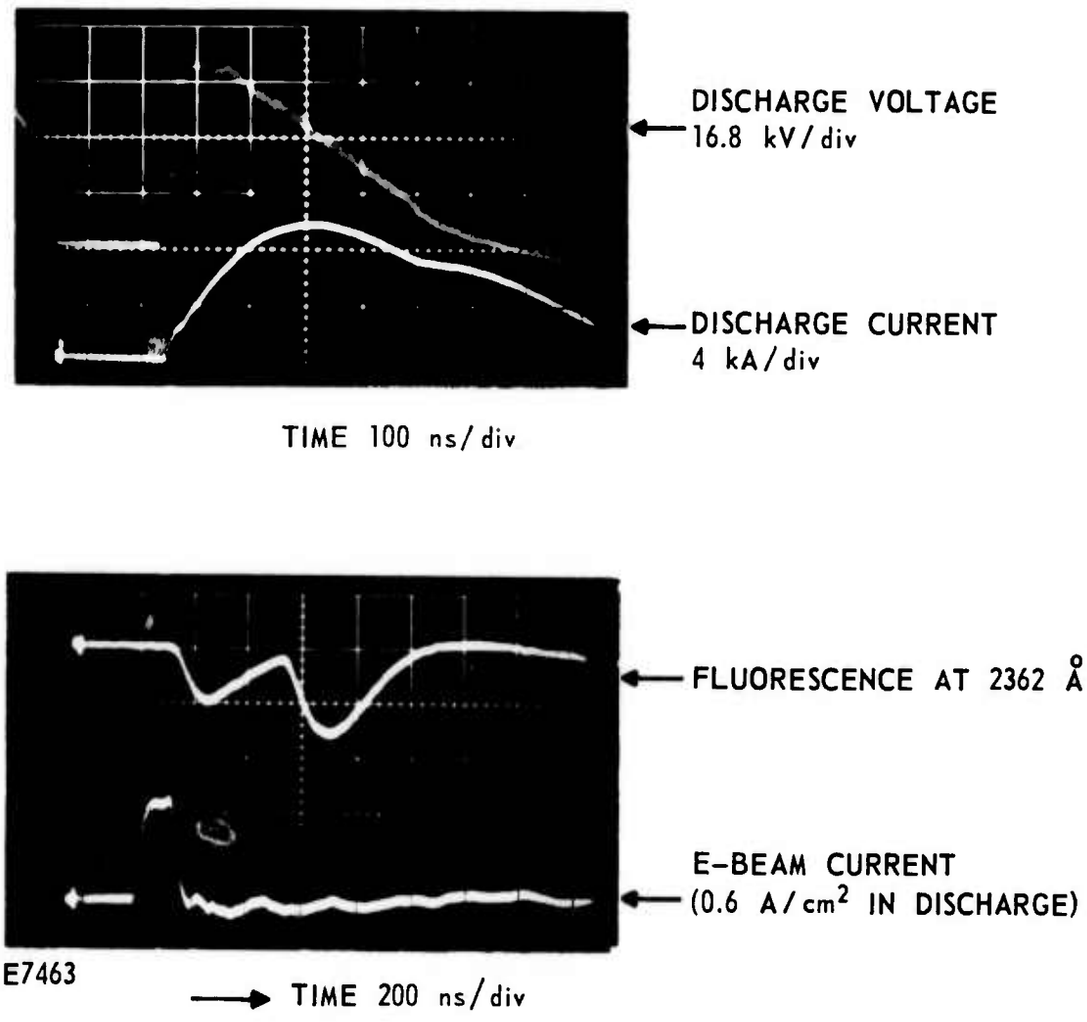

Figure 14 Experimental Results in N_2/NO Discharge

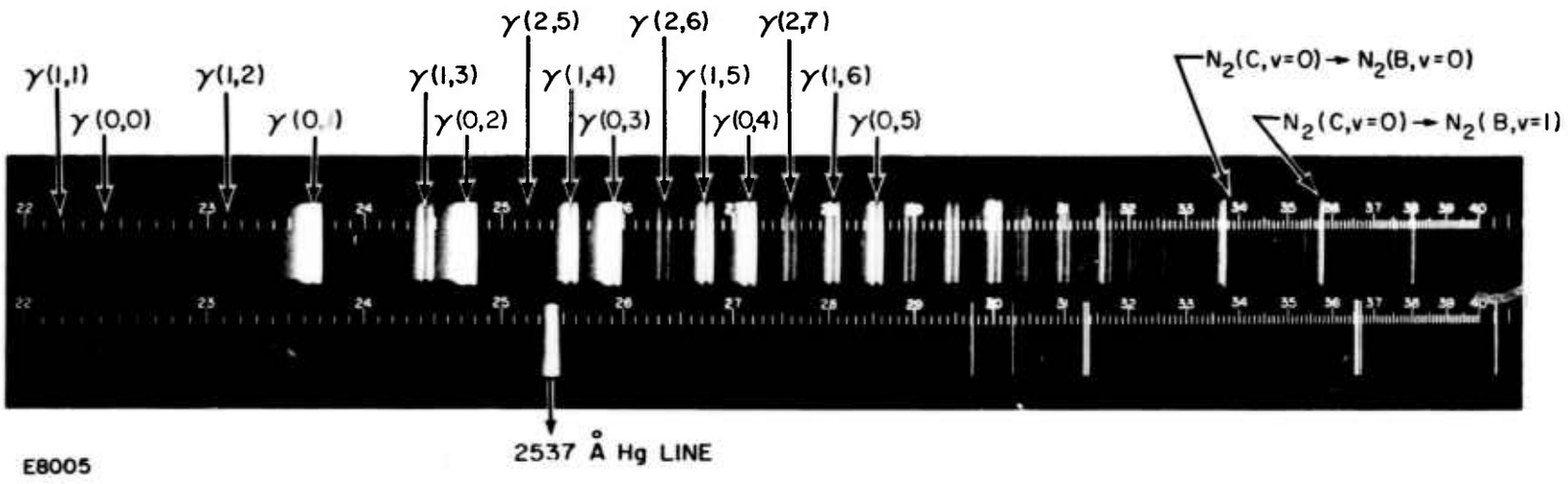

Figure 15 Time Averaged Spectrum of Light From an N_2/NO Discharge. Partial pressure of NO was 3 torr in an atmosphere of N_2. Also shown in a Hg spectrum.

by using the Boltzmann code if all the electron impact cross sections of SF_6 were known. Figure 16 shows the predictions of the Boltzmann code when 2 torr of SF_6 is added to a 97% Ar/3%N_2 mix. In the calculation we have only included the affects of attachment and ionization for SF_6. We should point out that the vibrational and electronic cross sections of SF_6 are not known and so they are not included in the Boltzmann code at this time. On comparing Figure 15 with Figure 10 we find that the only significant difference obtained by adding SF_6 is that we now have no net ionization at electric fields as high as 10.8 kV/cm atm. The percentage of discharge energy into Ar^* is essentially unchanged.

Figure 17 shows the experimental results for such a mixture. The discharge electric field was 8.5 - 9 kV/cm atm and the discharge current was almost square-topped. In fact, there was no arc. The energy input was about 23 J/liter which is an order of magnitude enhancement over the same mix without SF_6. Figure 18 shows the result of increasing the electric field to about 15 kV/cm atm. The discharge current exponentiates and discharge arcs after about 70 nsec. Appoximately 16 J/liter was depostied in the laser mixture during the stable portion of the discharge pulse. Comparison of Figures 17 and 18 shows that the E/P at which ionization is balanced by attachment occurs between 9 kV/cm atm and 15 kV/cm atm as predicted by the Bolzmann code.

E. PRELIMINARY Ar/N_2 AND $Ar/N_2/SF_6$ LASER EXPERIMENTS

Preliminary Ar/N_2 laser experiments involved an attempt at generating the N_2 (C, v = 0) to N_2 (B, v = 1) flourescence level required for laser onset. The threshold fluorescence level in our optical cavity (stable resonator output coupling 5%, gain length 20 cm, distance between mirrors 70 cm) was determined by first pumping the Ar/N_2 laser directly with the e-beam only. By attenuating the e-beam current density we found that the threshold for lasing occurred with an e-beam current density of ~ 6 A/cm^2. By blocking one of the cavity mirrors the threshold fluorescence level (in relative units) could be established. The e-beam current density was then attenuated by an additional factor of 10 and a discharge was generated in the ionization created by the beam. The discharge was delayed up to 1 μ sec with respect to the end of the e-beam pulse. At low electric fields ($\leq$ 5 kV/cm atm) no enhancement of 3577 Å flourescence was observed over that obtained with the 0.6 A/cm^2 e-beam. At higher electric fields, efficient enhancement of the 3577 Å radiation was observed in both Ar/N_2 and $Ar/N_2/SF_6$ mixtures. However the flourescence in each case saturated just below the threshold for laser action by e-beam pumping. We feel that the probable cause is metastable ionization. It takes 11.5 eV and more to excite Ar^* and it requires only another 4 eV or less to ionize the metastable. In the case of Ar/N_2 this additional ionization make the discharge more susceptible to arcing. However the argon ions so formed are eventually channeled back to Ar^* as discussed previously. There is a slight loss in efficiency because of the energy required to ionize Ar^*. With the addition of SF_6 the enhanced ionization rate, caused by Ar^* ionizations, can be balanced by attachment. However now the ionized Ar^* aren't channeled back by dissociative recombination because the discharge electrons are attached by SF_6.

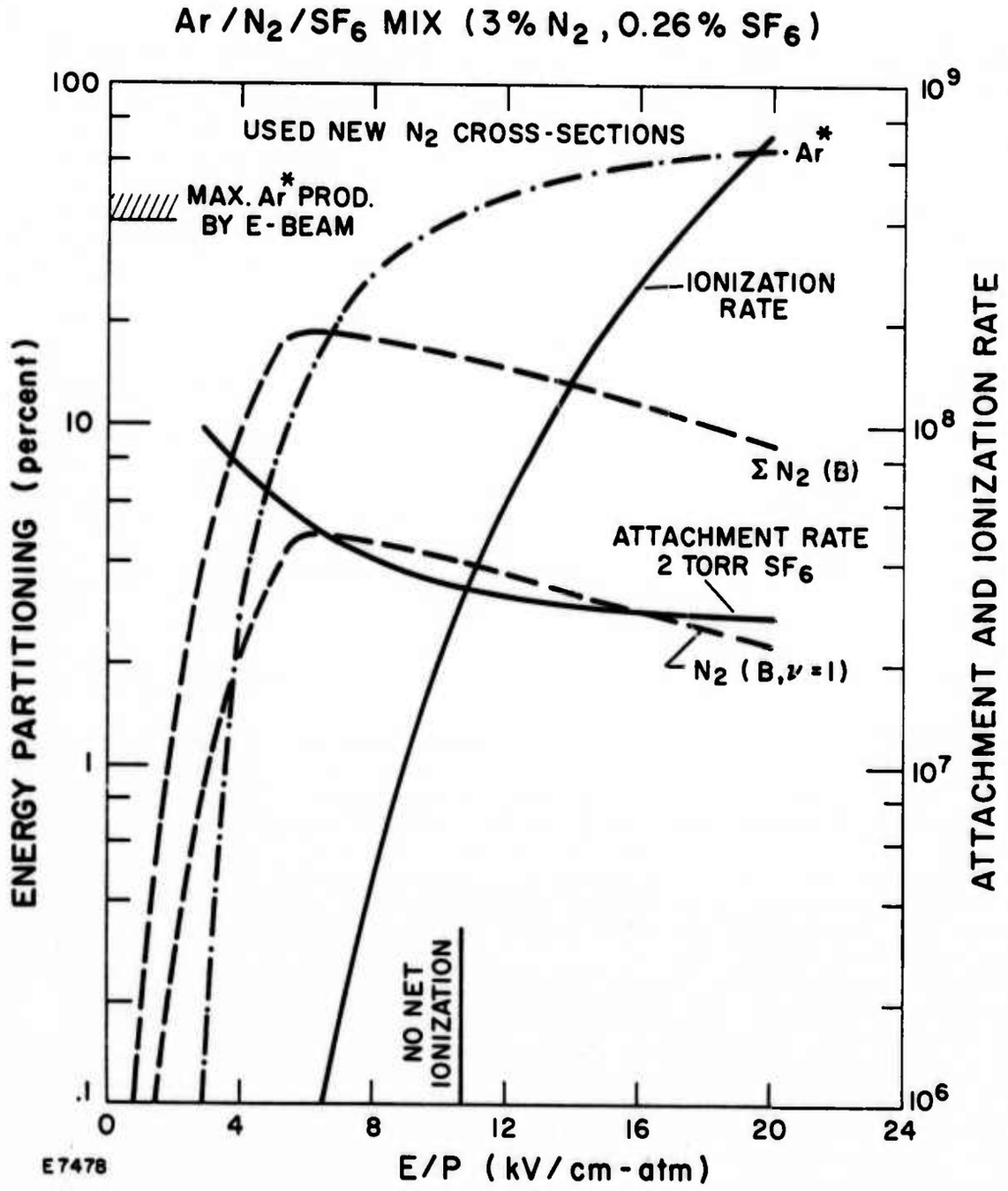

Figure 16 Fraction of Discharge Energy Into Various Excited States of Ar and N_2 for $Ar/N_2/SF_6$ Mixture. Notice that for E/p's up to 10.8 kV/cm atm there is no net ionization rate.

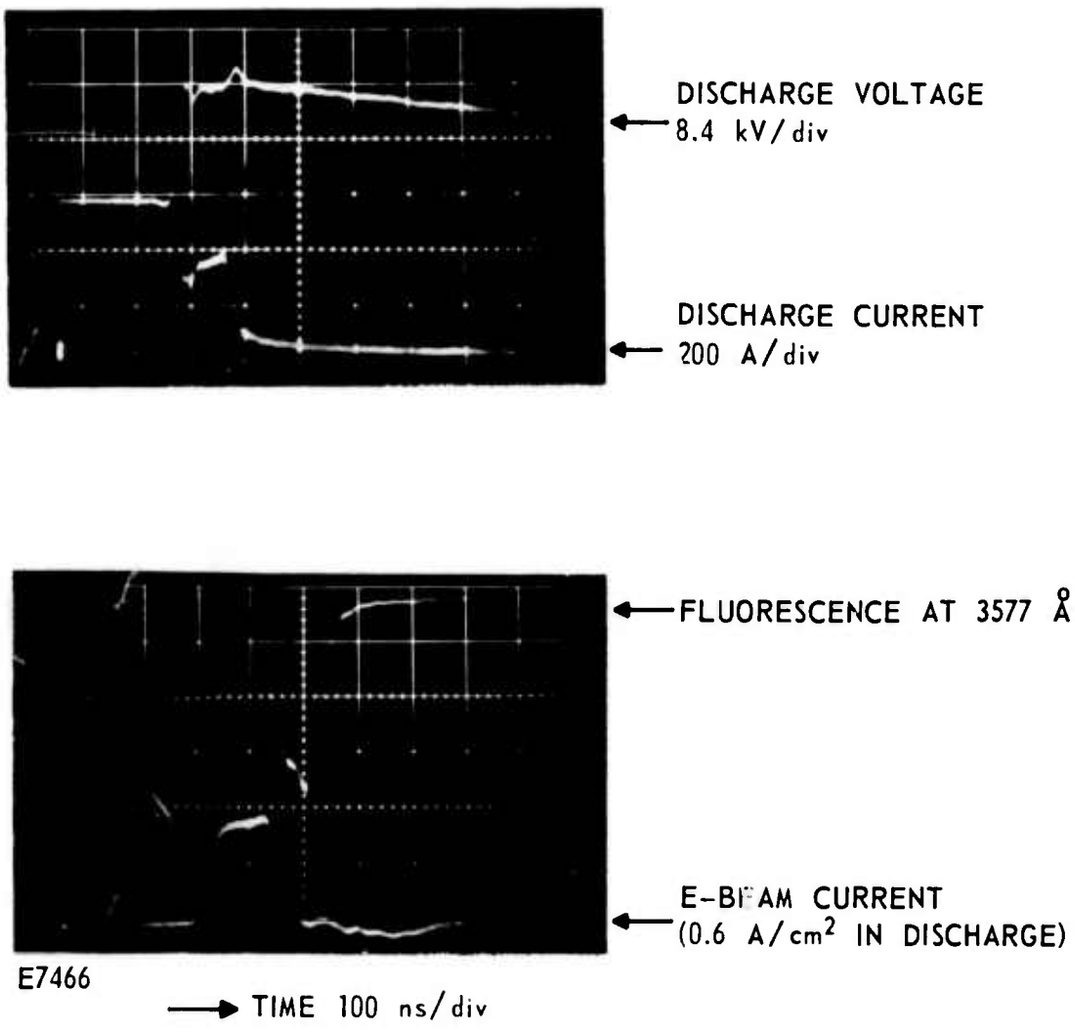

Figure 17 Experimental Results in $Ar/N_2/SF_6$

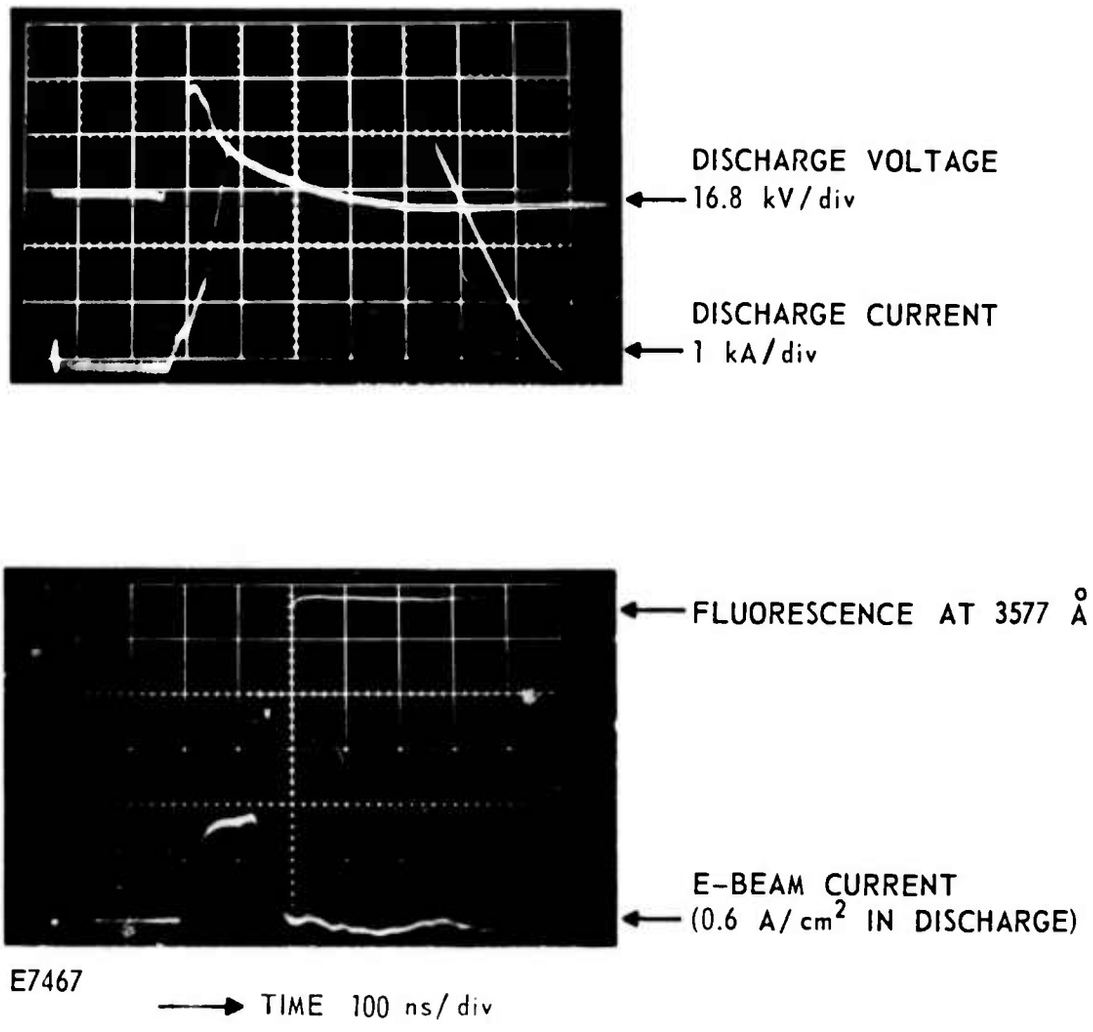

Figure 18 Experimental Results in $Ar/N_2/SF_6$

There are three possible methods of increasing the $N_2(C)$ population:

(i) Redesign of the discharge cavity. The results of our breakdown experiments together with the predictions of our electrostatics code indicate that straight wall insulators will have a higher standoff voltage capability. We expect that the pulsed breakdown characteristics will also be improved. If discharge operation at 10 kV/cm atm can be maintained for longer time periods, laser action should result. The new cavity will be built in FY76.

(ii) Increase the N_2 concentration. The Ar^* is quenched by N_2 every tenth collision so if the N_2 concentration is increased the loss rate for Ar^* is increased. As a result for a given input power the population of Ar^* will be smaller. Unfortunately N_2 also deactivates the upper laser level so the N_2 concentration cannot be increased indefinitely. However it appears that we can double the N_2 concentration from 3 to 6% before N_2 deactivation will begin to dominate.

(iii) Use other attachers: SF_6 might interfere with the laser kinetics in two ways. If the electron impact cross sections for exciting SF_6 vibrationally or electronically are $> 10^{-15}$ cm^2 they could alter the electron temperature. Another possibility is that SF_6 deactivates Ar^*. However for the concentrations of SF_6 used by us this rate would have to be gas kinetic if it is to be repsonsible for inhibiting laser action.

REFERENCES

1. Bhaumik, M. and Ault, E., IEEE J. Quant. El. 624, 10 (1974).

2. Searles, S., NRL, to appear in App. Phys. Lett.

3. Ewing, J.J. and Yatsiv, S., Avco Everett Research Laboratory, Inc. LAR Proposal (1972).

4. Suchard, S., Aerospace, private communication.

5. Mangano, J.A., Avco Everett Research Laboratory, Inc. LAR Final Report (1973).

6. Cobine, J.D., Gaseous Conductors, Dover Pub., p. 166 (1957).

7. MacDonald, A.D., Microwave Breakdown in Gases, Wiley Pub., p. 25 (1966).

8. Olmsted, J., Newton, A.S. and Street, I.E., J. Chem. Phys. 42, 2321 (1965).

9. Golden, D.E., Fisher, L.H., Phys. Rev. 123, 1079 (1961).

10. Rapp, D., Englander-Golden, P., J. Chem. Phys. 43, 1464 (1965).

DISTRIBUTION LIST

Office of Naval Research, Department of the Navy, Arlington, VA 22217 - Attn: Physics Program (3 copies)

Naval Research Laboratory, Department of the Navy, Washington, D.C. 20375 - Attn: Technical Library (1 copy)

Office of the Director of Defense, Research and Engineering, Information Office Library Branch, The Pentagon, Washington, D.C. 20301 (1 copy)

U.S. Army Research Office, Box CM, Duke Station, Durham, N.C. 27706 (1 copy)

Defense Documentation Center, Cameron Station, Alexandria, VA 22314 (12 copies)

Defense Information Analysis Center, Battelle Memorial Institute, 505 King Avenue, Columbus, OH 43201 (1 copy)

Commanding Officer, Office of Naval Research Branch Office, 536 South Clark Street, Chicago, IL 60615 (1 copy)

New York Area Office, Office of Naval Research, 715 Broadway (5th Floor), New York, NY 10003 - Attn: Dr. Irving Rowe (1 copy)

San Francisco Area Office, Office of Naval Research, 760 Market Street, Room 447, San Francisco, CA 94102 (1 copy)

Air Force Office of Scientific Research, Department of the Air Force, Washington, D.C. 22209 (1 copy)

Office of Naval Research Branch Office, 1030 East Green Strast, Pasadena, CA 91106 - Attn: Dr. Robert Behringer (1 copy)

Code 102 IP (ONRL), Office of Naval Research, 300 N. Quincy Street, Arlington, VA 22217 (6 copies)

Defense Advanced Research Projects Agency, 1400 Wilson Blvd., Arlington, VA 22209 - Attn: Strategic Technology Office (1 copy)

Office Director of Defense, Research & Engineering, The Pentagon, Washington, D.C. 20301 - Attn: Assistant Director (Space and Advanced Systems) (1 copy)

Office of the Assistant Secretary of Defense, System Analysis (Strategic Programs), Washington, D.C. 20301 - Attn: Mr. Gerald R. McNichols (1 copy)

U.S. Arms Control and Disarmament Agency, Dept. of State Bldg., Rm. 4931, Washington, D.C. 20451 - Attn: Dr. Charles Henkin (1 copy)

Energy Research Development Agency, Division of Military Applications, Washington, D.C. 20545 (1 copy)

National Aeronautics and Space Administration, Lewis Research Center, Cleveland, OH 44135 - Attn: Dr. John W. Dunning, Jr. (1 copy) (Aerospace Res. Engineer)

National Aeronautics & Space Administration, Code RR, FOB 10B, 600 Independence Ave., SW, Washington, D.C. 20546 (1 copy)

National Aeronautics and Space Administration, Ames Research Center, Moffett Field, CA 94035 - Attn: Dr. Kenneth W. Billman (1 copy)

Department of the Army, Office of the Chief of RD&A, Washington, D.C. 20310 - Attn: DARD-DD (1 copy)
DAMA-WSM-T (1 copy)

Department of the Army, Office of the Deputy Chief of Staff for Operations & Plans, Washington, D.C. 20310 - Attn: DAMO-RQD - (1 copy)

Ballistic Missile Defense Program Office (BMDPO), The Commonwealth Building, 1300 Wilson Blvd., Arlington, VA 22209 - Attn: Mr. Albert J. Bast, Jr. (1 copy)

U.S. Army Missile Command, Research & Development Division, Redstone Arsenal, AL 35809 - Attn: Army High Energy Laser Programs (2 copies)

Commander, Rock Island Arsenal, Rock Island, IL 61201, Attn: SARRI-LR, Mr. J.W. McGarvey (1 copy)

Commanding Officer, U.S. Army Mobility Equipment R&D Center, Ft. Belvoir, VA 22060 - Attn: SMEFB-MW (1 copy)

Commander, U.S. Army Armament Command, Rock Island, IL 61201 - Attn: AMSAR-RDT (1 copy)

Director, Ballistic Missile Defense Advanced Technology Center, P.O. Box 1500, Huntsville AL 35807 - Attn: ATC-O (1 copy)
ACT-T (1 copy)

Commander, U.S. Army Material Command, Alexandria, VA 22304 - Attn: Mr. Paul Chernoff (AMCRD-T) (1 copy)

Commanding General, U.S. Army Munitions Command, Dover, NH 17801 - Attn: Mr. Gilbert F. Chasnov (AMSMU-R) (1 copy)

Director, U.S. Army Ballistics Res. Lab, Aberdeen Proving Ground, MD 21005 - Attn: Dr. Robert Eichenberger (1 copy)

Commandant, U.S. Army, Air Defense School, Ft. Bliss, TX 79916 - Attn: Air Defense Agency (1 copy)
ATSA-CTD-MS (1 copy)

Commanding General, U.S. Army Combat Dev. Command, Ft. Belvoir, VA 22060 - Attn: Director of Material, Missile Div. (1 copy)

Commander, U.S. Army Training & Doctrine Command, Ft. Monroe, VA 23651 - Attn: ATCD-CF (1 copy)

Commander, U.S. Army Frankford Arsenal, Philadelphia, PA 19137 - Attn: Mr. M. Elnick SARFA-FCD Bldg. 201-3 (1 copy)

Commander, U.S. Army Electronics Command, Ft. Monmouth, NJ 07703 - Attn: AMSEL-CT-L, Dr. R.G. Buser (1 copy)

Commander, U.S. Army Combined Arms Combat Development Activity, Ft. Leavenworth, KS 66027 (1 copy)

National Security Agency, Ft. Geo. G. Meade, MD 20755 - Attn: R.C. Foss A763 (1 copy)

Deputy Commandant for Combat & Training Development, U.S. Army Ordnance Center and School, Aberdeen Proving Ground, MD 21005
Attn: ATSL-CTD-MS-R (1 copy)

Commanding Officer, USACDC CBR Agency, Ft. McClellan, AL 36201 - Attn: CDCCBR-MR (Mr. F.D. Poer) (1 copy)

DISTRIBUTION LIST (Continued)

Department of the Navy, Office of the Chief of Naval Operations, The Pentagon 5C739, Washington, D.C. 20350 - Attn: (OP 982F3) (1 copy)

Office of Naval Research Branch Office, 495 Summer Street, Boston, MA 02210 - Attn: Dr. Fred Quelle (1 copy)

Department of the Navy, Deputy Chief of Navy Material (Dev.), Washington, D.C. 20360 - Attn: Mr. R. Gaylord (MAT 032B) (1 copy)

Naval Missile Center, Point Mugu, CA 93042 - Attn: Gary Gibbs (Code 5352) (1 copy)

Naval Research Laboratory, Washington, D.C 20375 - Attn: (Code 5503-EOTPO) (1 copy)
Dr. P. Livingston - Code 5560 (1 copy)
Dr. A. I. Schindler - Code 6000 (1 copy)
Dr. H. Shenker - Code 5504 (1 copy)
Mr. D.J. McLaughlin - Code 5560 (1 copy)
Dr. John L. Walsh - Code 5503 (1 copy)

High Energy Laser Project Office, Department of the Navy, Naval Sea Systems Command, Washington, D.C. 20360 - Attn: Capt. A. Skoln.ck, USN (PM 22) (1 copy)

Superintendent, Naval Postgraduate School, Monterey, CA 93940 - Attn: Library (Code 2124) (1 copy)

Navy Radiation Technology, Air Force Weapons Lab (NLO), Kirtland AFB, NM 87117 (1 copy)

Naval Surface Weapons Center, White Oak, Silver Spring, MD 20910 - Attn: Dr. Leon H. Schindel (Code 310) (1 copy)
Dr. E. Leroy Harris (Code 313) (1 copy)
Mr. K. Enkenhaus (Code 034) (1 copy)
Mr. J. Wise Code 047) (1 copy)
Technical Library (1 copy)

U.S. Naval Weapons Center, China Lake, CA 93555 - Atn: Technical Library (1 copy)

HQ USAF (AF/RDPS), The Pentagon, Washington, D.C. 20330 - Attn: Lt. Col. A.J. Chiota (1 copy)

HQ AFSC/XRLW, Andrews AFB, Washington, D.C. 20331 - Attn: Maj. J.M. Walton (1 copy)

HQ AFSC (DLCAW), Andrews AFB, Washington, D.C. 20331 - Attn: Maj. H. Axelrod (1 copy)

Air Force Weapons Laboratory, Kirtland AFB, NM 87117 - Attn: LR (1 copy)
AL (1 copy)

HQ SAMSO (XRTD), P.O. Box 92960, Worldway Postal Center, Los Angeles, CA 90009 - Attn: Lt. Dorian DeMaio (XRTD) (1 copy)

AF Avionics Lab (TEO), Wright Patterson AFB, OH 45433 - Attn: Mr. K. Hutchinson (1 copy)

Dept. of the Air Force, Air Force Materials Lab. (AFSC), Wright Patterson AFB, OH 45433 - Attn: Maj. Paul Elder (LPS) (1 copy)
Laser Window Group

HQ Aeronautical Systems Div., Wright Patterson AFB, OH 45433 - Attn: XRF - Mr. Clifford Fawcett (1 copy)

Rome Air Development Command, Griffiss AFB, Rome, NY 13440 - Attn: Mr. R. Urtz (OCSE) (1 copy)

HQ Electronics Systems Div. (ESL), L.G. Hanscom Field, Bedford, MA 01730 - Attn: Mr. Alfred E. Anderson (XRT) (1 copy)
Technical Library (1 copy)

Air Force Rocket Propulsion Lab., Edwards AFB, CA 93523 - Attn: B.R. Bornhorst, (LKCG) (1 copy)

Air Force Aero Propulsion Lab., Wright Patterson AFB, OH 45433 - Attn: Col. Walter Moe (CC) (1 copy)

Dept. of the Air Force, Foreign Technology Division, Wright Patterson AFB, OH 45433 - Attn: PDTN (1 copy)

Commandant of the Marine Corps, Scientific Advisor (Code RD-1), Washington, D.C. 20380 (1 copy)

Aerospace Research Labs., (AFSC), Wright Patterson AFB, OH 45433 - Attn: Lt. Col. Max Duggins (1 copy)

Defense Intelligence Agency, Washington, D.C. 20301 - Attn: Mr. Seymour Berler (DT1B) (1 copy)

Central Intelligence Agency, Washington, D.C. 20505 - Attn: Mr. Julian C. Nall (1 copy)

Analytic Services, Inc., 5613 Leesburg Pike, Falls Church, VA 22041 - Attn: Dr. John Davis (1 copy)

Aerospace Corp., P.O. Box 92957, Los Angeles, CA 90009 - Attn: Dr. G.P. Millburn (1 copy)

Airasaarch Manuf. Co., 9851-9951 Sepulveda Blvd., Los Angeles, CA 90009 - Attn: Mr. A. Colin Stancliffe (1 copy)

Atlantic Research Corp., Shirley Highway at Edsall Road, Alexandria, VA 22314 - Attn: Mr. Robert Naismith (1 copy)

Avco Everett Research Lab., 2385 Revere Beach Parkway, Evarett, MA 02149 - Attn: Dr. George Sutton (1 copy)
Dr. Jack Daugherty (1 copy)

Battelle Columbus Laboratories, 505 King Avenue, Columbus, OH 43201 - Attn: Mr. Fred Tietzel (STPIAC) (1 copy)

Bell Aerospace Co., Buffalo, NY 14240 - Attn: Dr. Wayne C. Solomon (1 copy)

Boeing Company, P.O. Box 3999, Seattle, WA 98124 - Attn: Mr. M.L. Gamble (2-, 460, MS 8C-88) (1 copy)

Electro-Optical Systems, 300 N. Halstead, Pasadena, CA 91107 - Attn: Dr. Andrew Jensen (1 copy)

ESL, Inc., 495 Java Drive, Sunnyvale, CA 94086 - Attn: Arthur Einhorn (1 copy)

DISTRIBUTION LIST (Continued)

Generel Electric Co., Space Division, P.O. Box 8555, Philedelphie, PA 19101 - Attn: Dr. R.R. Sigismonti (1 copy)

Generel Electric Co., 100 Plestics Avenue, Pittsfield, MA 01201 - Attn: Mr. D.G. Herrington (Rm. 1044) (1 copy)

Generel Reseerch Corp., P.O. Box 3587, Senta Barbara, CA 93105 - Attn: Dr. R. Holbrook (1 copy)

General Reseerch Corp., 1501 Wilson Blvd., Suite 700, Arlington, VA 22209 - Attn: Dr. Giles F. Crimi (1 copy)

Hercules, Inc., Industrial System Dept., Wilmington, DE 19899 - Attn: Dr. R.S. Voris (1 copy)

Hercules, Inc., P.O. Box 210, Cumberlend, MD 21502 - Attn: Dr. Ralph R. Preckel (1 copy)

Hughes Reseerch Lebs., 3011 Melibu Cenyon Roed, Malibu, CA 90265 - Attn: Dr. D. Forster (1 copy)

Hughes Aircreft Co., Aerospece Group - Systems Division, Cenoga Perk, CA 91304 - Attn: Dr. Jeck A. Alcalay (1 copy)

Hughes Aircreft Co., Centinele end Teele Streets, Bldg. 6, MS E-125, Culver City, CA 90230 - Attn: Dr. William Yates (1 copy)

Institute for Defense Analyses, 400 Army-Navy Drive, Arlington, VA 22202 - Attn: Dr. Alvin Schnitzler (1 copy)

Johns Hopkins University, Applied Physics Lab., 8621 Georgia Avenue, Silver Spring, MD 20910 - Attn: Dr. Albert M. Stone (1 copy)

Lewrence Livermore Laboretory, P.O. Box 808, Livermore, CA 94550 - Attn: Dr. R.E. Kidder (1 copy)
Dr. E. Teller (1 copy)
Dr. Jos Fleck (1 copy)

Los Alemos Scientific Leboretory, P.O. Box 1663, Los Alemos, NM 87544 - Attn: Dr. Keith Boyer (1 copy)

Lulejien end Associetes, Inc., Del Amo Finenciel Center, 21515 Hewthorne Blvd. - Suite 500, Torrence, CA 90503 (1 copy)

Lockheed Palo Alto Res. Leb., 3251 Henover St., Pelo Alto, CA 94303 - Attn: L.R. Lunsford, Orgn. 52-24, Bldg. 201 (1 copy)

Mathematicel Sciences Northwest, Inc., P.O. Box 1887, Bellevue, WN 98009 - Attn: Dr. Abreham Hertsberg (1 copy)

Mertin Merietta Corp., P.O. Box 179, Meil Stetion 0471, Denver, CO 80201 - Attn: Mr. Stewert Chepin (1 copy)

Massachusetts Institute of Technology, Lincoln Leboratory, P.O. Box 73, Lexington, MA 02173 - Attn: Dr. S. Edelberg (1 copy)
Dr. L.C. Marquet (1 copy)

McDonnell Douglas Astroneutics Co., 5301 Bolse Avenue, Huntington Beach, CA 92647 - Attn: Mr. [illegible] L. Klevatt, Dept. A3-830-BBFO, M/S 9 (1 copy)

McDonnell Douglas Research Labs., Dept. 220, Box 516, St. Louis, MO 63166 - Attn: Dr. D.P. Ames (1 copy)

MITRE Corp., P.O. Box 208, Bedford, MA 01730 - Attn: Mr. A.C. Cron (1 copy)

North Americen Rockwell Corp., Autonetics Div., Aneheim, CA 92803 - Attn: Mr. T.T. Kumagi, C/476 Mail Code HA18 (1 copy)

Northrop Corp., 3401 West Broedwey, Hawthorne, CA 90250 - Attn: Dr. Gererd Hasserjian, Leser Systems Dept. (1 copy)

Dr. Anthony N. Pirri, Physical Sciences, Inc., 18 Lakeside Office Perk, Wakefield, MA 01880 (1 copy)

RAND Corp., 1700 Mein Street, Senta Monice, CA 90406 - Attn: Dr. C.R. Culp/Mr. G.A. Center (1 copy)

Raytheon Co., 28 Seyon Street, Weltham, MA 02154 - Attn: Dr. F.A. Horrigen (Res. Div.) (1 copy)

Reytheon Co., Boston Post Roed, Sudbury, MA 01776 - Attn: Dr. C. Sonnenschien (Equip. Div.) (1 copy)

Raytheon Co., Bedford Lebs, Missile Systems Div., Bedford, MA 01730 - Attn: Dr. H.A. Mehlhorn (1 copy)

Riverside Reseerch Institute, 80 West End Street, New York, NY 10023 - Attn: Dr. L.H. O'Neill (1 copy)
Dr. John Bose (1 copy)
(HPEGL Library) (1 copy)

R&D Associates, Inc., P.O. Box 3580, Sente Monice, CA 90431 - Attn: Dr. R.E. LeLevier (1 copy)

Rockwell Internetionel Corporation, Rocketdyne Division, Albuquerque District Office, 3636 Meneul Blvd., NE, Suite 211, Albuquerque, NM 87110 - Attn: C.K. Kraus, Mgr. (1 copy)

SANDIA Corp., P.O. Box 5800, Albuquerque, NM 87115 - Attn: Dr. Al Nerath (1 copy)

Stanford Reseerch Institute, Menlo Perk, CA 94025 - Attn: Dr. F.T. Smith (1 copy)

Science Applications, Inc., 1911 N. Ft. Meyer Drive, Arlington, VA 22209 - Attn: L. Peckam (1 copy)

Science Applications, Inc., P.O. Box 328, Ann Arbor, MI 48103 - Attn: R.E. Meredith (1 copy)

Sciences Applicetions, Inc., 6 Preston Court, Bedford, MA 01703 - Attn: R. Greenberg (1 copy)

Science Applications, Inc., P.O. Box 2351, La Jolla, CA 92037 - Attn: Dr. John Asmus (1 copy)

Systems, Sciences and Software, P.O. Box 1620, La Jolla, CA 92037 - Attn: Alen F. Klein (1 copy)

Systems Consultants, Inc., 1050 31st Street, NW, Washington, D.C. 20007 - Attn: Dr. R.B. Keller (1 copy)

Thiokol Chemical Corp., WASATCH Division, P.O. Box 524, Brigham City, UT 84302 - Attn: Mr. J.E. Hansen (1 copy)

TRW Systems Group, One Space Park, Bldg. R-1, Rm. 1050, Redondo Beach, CA 90278 - Attn: Mr. Norman Campbell (1 copy)

United Technologies Reseerch Center, 400 Main Street, East Hartford, CT 06108 - Attn: Mr. G.H. McLafferty (3 copies)

DISTRIBUTION LIST (Continued)

United Technologies Research Center, Pratt and Whitney Aircraft Div., Florida R&D Center, West Palm Beach, FL 33402 Attn: Dr. R.A. Schmidtke (1 copy)
Mr. Ed Pinsley (1 copy)

VARIAN Associates, EIMAC Division, 301 Industrial Way, San Carlos, CA 94070 - Attn: Mr. Jack Quinn (1 copy)

Vought Systems Division, LTV Aerospace Corp., P.O. Box 5907, Dallas, TX 75222 - Attn: Mr. F.G. Simpson, MS 254142 (1 copy)

Westinghouse Electric Corp., Defense and Space Center, Balt-Wash. International Airport - Box 746, Baltimore, MD 21203 - Attn: Mr. W.F. List (1 copy)

Westinghouse Research Labs., Beulah Road, Churchill Boro, Pittsburgh, PA 15235 - Attn: Dr. E.P. Riedel (1 copy)

United Technologies Research Center, East Hartford, CT 06108 - Attn: A.J. DeMaria (1 copy)

Airborne Instruments Laboratory, Walt Whitorian Road, Melville, NY 11746 - Attn: F. Pace (1 copy)

General Electric R&D Center, Schenectady, NY 12305 - Attn: Dr. Donald White (1 copy)

Cleveland State University, Cleveland, OH 44115 - Attn: Dean Jack Soules (1 copy)

EXXON Research and Engineering Co., P.O. Box 8, Linden, NJ 07036 - Attn: D. Grafstein (1 copy)

University of Maryland, Department of Physics and Astronomy, College Park, MD 20742 - Attn: D. Currie (1 copy)

Sylvania Electric Products, Inc., 100 Fergeson Drive, Mountain View, CA 94040 - Attn: L.M. Osterink (1 copy)

North American Rockwell Corp., Autonetics Division, 3370 Miraloma Avenue, Anaheim, CA 92803 - Attn: R. Gudmundsen (1 copy)

Massachusetts Institute of Technology, 77 Massachusetts Avenue, Cambridge, MA 02138 - Attn: Prof. A. Javan (1 copy)

Lockheed Missile & Space Co., Palo Alto Research Laboratories, Palo Alto, CA 94304 - Attn: Dr. R.C. Ohlman (1 copy)

ILC Laboratories, Inc., 164 Commercial Street, Sunnyvale, GA 94086 - Attn: L. Noble (1 copy)

University of Texas at Dallas, P.O. Box 30365, Dallas, TX 75230 - Attn: Prof. Carl B. Collins (1 copy)

Polytechnic Institute of New York, Rt. 110, Farmingdale, NY 11735 - Attn: Dr. William T. Walter (1 copy)